Brassinosteroids Antagonize Jasmonate-Activated Plant Defense Responses through BRI1-EMS-SUPPRESSOR1 (BES1)[1]

Ke Liao,[a,2] Yu-Jun Peng,[a,2] Li-Bing Yuan,[a,2] Yang-Shuo Dai,[a,2] Qin-Fang Chen,[a] Lu-Jun Yu,[a] Ming-Yi Bai,[b] Wen-Qing Zhang,[a] Li-Juan Xie,[a,3] and Shi Xiao[a,3,4]

[a]State Key Laboratory of Biocontrol, Guangdong Provincial Key Laboratory of Plant Resources, School of Life Sciences, Sun Yat-sen University, Guangzhou 510275, China
[b]School of Life Sciences, Shandong University, Jinan 250110, China

ORCID IDs: 0000-0001-5303-8676 (L.-B.Y.); 0000-0001-8996-4030 (Y.-S.D.); 0000-0001-5992-7511 (M.-Y.B.); 0000-0001-5721-5908 (L.-J.X.); 0000-0002-6632-8952 (S.X.).

Brassinosteroids (BRs) and jasmonates (JAs) regulate plant growth, development, and defense responses, but how these phytohormones mediate the growth-defense tradeoff is unclear. Here, we identified the Arabidopsis (*Arabidopsis thaliana*) *dwarf at early stages1* (*dwe1*) mutant, which exhibits enhanced expression of defensin genes *PLANT DEFENSIN1.2a* (*PDF1.2a*) and *PDF1.2b*. The *dwe1* mutant showed increased resistance to herbivory by beet armyworms (*Spodoptera exigua*) and infection by botrytis (*Botrytis cinerea*). *DWE1* encodes ROTUNDIFOLIA3, a cytochrome P450 protein essential for BR biosynthesis. The JA-inducible transcription of *PDF1.2a* and *PDF1.2b* was significantly reduced in the *BRASSINOSTEROID INSENSITIVE1-ETHYL METHANESULFONATE-SUPPRESSOR1* (*BES1*) gain-of-function mutant *bes1- D*, which was highly susceptible to *S. exigua* and *B. cinerea*. BES1 directly targeted the terminator regions of *PDF1.2a/PDF1.2b* and suppressed their expression. *PDF1.2a* overexpression diminished the enhanced susceptibility of *bes1- D* to *B. cinerea* but did not improve resistance of *bes1- D* to *S. exigua*. In response to *S. exigua* herbivory, BES1 inhibited biosynthesis of the JA-induced insect defense-related metabolite indolic glucosinolate by interacting with transcription factors MYB DOMAIN PROTEIN34 (MYB34), MYB51, and MYB122 and suppressing expression of genes encoding CYTOCHROME P450 FAMILY79 SUBFAMILY B POLYPEPTIDE3 (CYP79B3) and UDP-GLUCOSYL TRANSFERASE 74B1 (UGT74B1). Thus, BR contributes to the growth-defense tradeoff by suppressing expression of defensin and glucosinolate biosynthesis genes.

Plants have evolved an exquisite regulatory mechanism for defense against pathogens and pests. Phytohormones, including jasmonates (JAs), salicylic acid (SA), ethylene (ET), brassinosteroids (BRs), gibberellic acid (GA), abscisic acid (ABA), cytokinins (CKs), and auxin (AU), act as essential signals for the regulation of plant immune responses to microbial pathogens and insect herbivores (Pieterse et al., 2012; Ning et al., 2017). Among these, JAs, which include jasmonic acid and its cyclopentanone derivatives, are lipid-derived hormones that play primary roles in regulating plant defense responses (Wasternack and Hause, 2013; Zhang et al., 2017; Howe et al., 2018). In response to pathogen infection or insect feeding, plants rapidly accumulate JAs, thereby triggering large-scale transcriptional reprogramming of defense- and metabolism-associated genes, including genes encoding defensins, proteinase inhibitors, Thr deaminases, and enzymes involved in secondary metabolic pathways, such as for glucosinolate (GS) biosynthesis (Zhang et al., 2017; Wang et al., 2019).

JA-mediated defense responses require the F-box protein CORONATINE INSENSITIVE1 (COI1) for subsequent signal transduction in plant cells (Xie et al., 1998; Yan et al., 2009; Sheard et al., 2010). In Arabidopsis (*Arabidopsis thaliana*), COI1 forms an E3 ubiquitin ligase complex with Skp1/Cullin/F-box (SCF), which acts as a JA receptor (Xie et al., 1998; Xu et al., 2002; Xiao et al., 2004). The JA-SCF^{COI1} complex promotes interactions with jasmonate-ZIM domain (JAZ) transcriptional repressors (Xie et al., 1998; Thines et al., 2007; Katsir et al., 2008). These hormone-dependent interactions lead to the ubiquitination and degradation of JAZ suppressors by the 26S proteasome, thereby activating JA-responsive

[1]This work was supported by the National Natural Science Foundation of China (projects 31725004 and 31670276 to S.X., project 31700220 to L.-J.X., project 31800232 to Y.-S.D., and project U1401212 to W.-Q.Z.), the Natural Science Foundation of Guangdong Province, China (project 2017A030308008 to S.X.), the China Postdoctoral Science Foundation (project 2018M633213 to L.-B.Y. and project 2018M633232 to Y.-S.D.), and Sun Yat-sen University (projects 17lgpy110 and PlantKF02 to L.-J.X.).

[2]These authors contributed equally to the article.

[3]Senior authors.

[4]Author for contact: xiaoshi3@mail.sysu.edu.cn.

The author responsible for distribution of materials integral to the findings presented in this article in accordance with the policy described in the Instructions for Authors (www.plantphysiol.org) is: Shi Xiao (xiaoshi3@mail.sysu.edu.cn).

S.X. designed the research; K.L., Y.-J.P., L.-B.Y., Y.-S.D., Q.-F.C., and L.-J.Y. carried out the experiments; S.X., M.-Y.B., W.-Q.Z., and L.-J.X. analyzed the data; S.X., L.-J.X., and K.L. wrote the manuscript.

www.plantphysiol.org/cgi/doi/10.1104/pp.19.01220

gene expression (Chini et al., 2007; Thines et al., 2007; Chung and Howe, 2009). In general, two types of transcriptional activators are involved in downstream transcriptional reprogramming in the JAZ-mediated JA signaling pathway (Zhang et al., 2017). First, the APETALA2/ETHYLENE RESPONSE FACTOR (AP2/ERF) family members ERF1 and OCTADECANOID-RESPONSIVE ARABIDOPSIS59 (ORA59) function in plant resistance to necrotrophic pathogens by modulating the expression of *PLANT DEFENSIN1.2* (*PDF1.2*; Pré et al., 2008; Zarei et al., 2011; Pieterse et al., 2012; Wasternack and Hause, 2013). Second, the MYC basic helix-loop-helix (bHLH) transcription factors, including MYC2/3/4/5, bHLH3/13/14/17, and the WD-repeat/bHLH/MYB complex, help regulate plant responses to wounding or herbivore attack (Zhai et al., 2013; Howe et al., 2018; Wang et al., 2019).

Much of the mechanism by which the JAZ-MYC transcriptional module controls plant responses to herbivore feeding has recently been elucidated using genetic and biochemical approaches. Specifically, the triple mutant *myc2/3/4* is extremely susceptible to generalist herbivores (Fernández-Calvo et al., 2011; Major et al., 2017), suggesting that MYC2, MYC3, and MYC4 have redundant roles in maintaining insect immunity in plants. Moreover, these MYC transcription factors activate GS biosynthesis by targeting the promoters of several GS biosynthesis genes or by forming a transcriptional complex with GS-related MYB factors, including MYB28 and MYB34 (Schweizer et al., 2013). GSs are a class of nitrogen- and sulfur-containing secondary metabolites that are catabolized into toxic compounds during plant interactions with herbivores (Schweizer et al., 2013; Wang et al., 2019).

BRs are a group of steroidal growth-promoting plant hormones with a wide range of effects on plant growth and development (Gudesblat and Russinova, 2011). Three pathways, including the early C-22 oxidation, early C-6 oxidation, and late C-6 oxidation pathways, function as a cascade for BR biosynthesis. During these processes, the cytochrome P450 ROTUNDIFOLIA3 (ROT3) plays an important role in controlling the conversion steps in the early C-6 or late C-6 oxidation pathways to generate active BR species (Choe, 2006). BR is perceived by the membrane-anchored receptor kinase BRASSINOSTEROID-INSENSITIVE1 (BRI1), which activates its coreceptor kinase, BRI1-ASSOCIATED RECEPTOR KINASE1 (BAK1), to inactivate the downstream GSK3-like kinase BRASSINAZOLE-INSENSITIVE2 (BIN2) through phosphorylation (Li et al., 2002). The transcription factors BRASSINAZOLE-RESISTANT1 (BZR1) and BRI1-EMS-SUPPRESSOR1 (BES1) function as master regulators downstream of BR signaling (Wang et al., 2002; Yin et al., 2002; Gampala et al., 2007). In response to BRs, the dephosphorylated BES1/BZR1 translocates into the nucleus to bind with the CGTGT/CG (BRRE) and CANNTG (E-box) motifs in the promoters of their target genes, thereby inducing or repressing target gene expression (Wang et al., 2012).

BRs are also actively involved in plant responses to diverse biotic and abiotic stresses (Nolan et al., 2017; Yu et al., 2018). In particular, the phosphorylation of Arabidopsis BES1 by MPK6 enhances plant resistance against the hemibiotrophic bacterium *Pseudomonas syringae* pv. *tomato* DC3000 (Kang et al., 2015). Indeed, the *bes1- D* mutant, which carries a dominant point mutation in BES1 (Yin et al., 2002), shows enhanced resistance to this bacterium but increased susceptibility to the necrotrophic fungus *Alternaria brassicicola* (Shin et al., 2016). BRs also play an important role in plant-herbivore interactions. In response to insect attack, BRs likely facilitate the negative regulation of GS biosynthesis by BES1 and/or BZR1 to achieve a tradeoff between growth and immunity (Guo et al., 2013; Yu et al., 2018). However, direct evidence for the roles of BRs in plant defense responses to pathogens and insect herbivory is currently lacking.

Here, we identified the knockout Arabidopsis mutant *dwarf at early stages1* (*dwe1*), which harbors a transfer DNA (T-DNA) insertion in the gene encoding ROT3, a cytochrome P450 family protein involved in BR biosynthesis. Interestingly, the *dwe1* (a new *rot3-4* allele) mutant shows increased resistance to the necrotrophic fungus *Botrytis cinerea* and the insect herbivore *Spodoptera exigua*. Biochemical analysis indicated that in response to pathogen infection or insect feeding, BES1 inhibits the transcription of genes involved in plant defensins and GS biosynthesis, respectively. This study provides strong evidence that the BR-JA interaction contributes to the plant growth-defense tradeoff in Arabidopsis.

RESULTS

Isolation and Characterization of *dwe1*

During a screening of Arabidopsis transgenic lines expressing the empty binary vector pSMB (Mylne and Botella, 1998), we obtained the T-DNA insertional mutant *dwe1*, which exhibits a semidwarf phenotype during early development (Fig. 1A). Compared to wild-type plants, 4-week-old *dwe1* plants have rounded leaves and shorter petioles (Fig. 1, A and B). Moreover, *dwe1* plants show delayed age-dependent leaf senescence compared to the wild type (Fig. 1C). Scanning electron microscopy (SEM) revealed clustered stomata on the surfaces of 3-week-old *dwe1* rosettes (Fig. 1D), and stomatal density was significantly higher in *dwe1* than in the wild type (Fig. 1E).

To investigate the biological function of *DWE1*, we performed microarray analysis using the rosettes of 4-week-old wild-type and *dwe1* plants grown under normal conditions. Compared to the wild type, 266 genes were differentially expressed by more than 1.5-fold in *dwe1*, including 122 upregulated and 144 downregulated genes (Supplemental Table S1). The *dwe1* mutation induced significant changes in the mRNA levels of genes involved in biotic/abiotic stress,

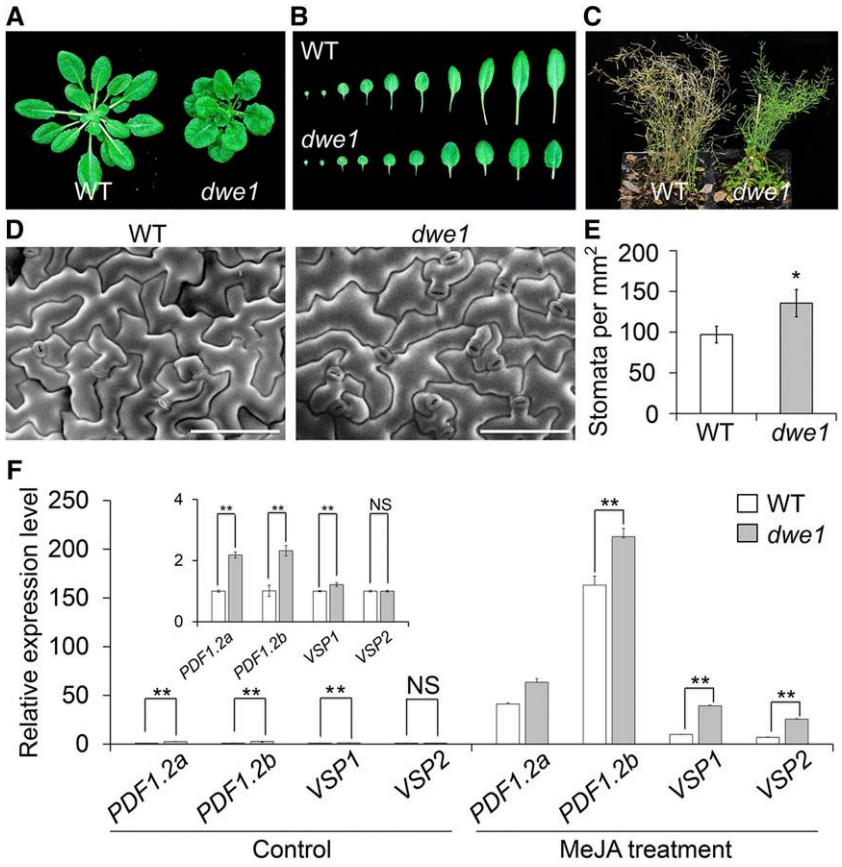

Figure 1. Isolation and phenotypic characterization of *dwe1*. A, Phenotypes of 4-week-old wild-type (WT) and *dwe1* plants. B, Morphology of wild-type and *dwe1* leaves. C, Senescent phenotypes of wild-type and *dwe1* mutant. D and E, Stomata on the leaves of 3-week-old wild-type and *dwe1* plants revealed by SEM (D) and calculation of stomatal densities (E). Experiments were repeated three times independently. For each experiment, five leaves from independent plants were used for each genotype. Error bars represent SD ($n = 5$). Asterisk indicates Student's *t* test significance between wild type and *dwe1* mutant ($^*P < 0.05$). Bars = 50 μm. F, Reverse transcription quantitative PCR (RT-qPCR) analysis of the JA-inducible genes *PDF1.2a*, *PDF1.2b*, *VSP1*, and *VSP2* in 6-d-old wild-type and *dwe1* seedlings treated without (control) or with MeJA treatment (100 μM MeJA) for 6 h. The expression levels of *PDF1.2s* and *VSPs* of plants harvested at 0 h are shown at the top left. The experiments were biologically repeated three times with similar results. For one experiment, three technical replicates (30 seedlings were pooled for each replicate) were used for each genotype. Error bars represent SD ($n = 3$ technical replicates). Asterisks indicate Student's *t*-test significance between indicated samples ($^{**}P < 0.01$ and $^*P < 0.05$). NS, no significant difference.

senescence, metabolism, transcription, transport, and signaling, as indicated by functional annotation (Supplemental Table S1). In particular, GO analysis revealed that GO:0009753 (response to jasmonic acid) was enriched in the differentially expressed genes (DEGs; Supplemental Fig. S1). Interestingly, the transcript levels of two genes, *PDF1.2a* and *PDF1.2b*, were particularly elevated (18.3- and 12.6-fold, respectively) in the *dwe1* mutant compared to the wild type. *PDF1.2a* and *PDF1.2b* encode plant defensins, which are widely used as downstream markers of JA signaling (Brown et al., 2003). Therefore, our findings suggest that the mutation of *DWE1* leads to altered JA-mediated signaling and defense responses.

To investigate this notion, we analyzed the expression levels of *PDF1.2a* and *PDF1.2b*, as well as two other JA marker genes, *VEGETATIVE STORAGE PROTEIN1* (*VSP1*) and *VSP2*, in wild-type and *dwe1* seedlings with or without 100 μM methyl jasmonate (MeJA) treatment. Under normal conditions, *PDF1.2a* and *PDF1.2b*, but not *VSP1* or *VSP2*, were significantly upregulated in *dwe1* compared to the wild type (Fig. 1F). The difference in gene expression levels between RT-qPCR and microarray data are likely due to the different sample ages and methods of data acquisition. All four genes were significantly induced in wild-type plants upon MeJA treatment and were further upregulated in *dwe1* (Fig. 1F), suggesting that DWE1 is involved in modulation of JA-associated defense genes in Arabidopsis.

The morphological abnormalities of *dwe1* plants resembled those of BR synthesis or signaling mutants (Li et al., 2002). To verify the role of DWE1 in BR pathway, we examined the effects of exogenous application of brassinolide (BL) on *dwe1* plants. When 4-week-old wild-type and *dwe1* plants were sprayed with 100 μM BL, the leaf shape and petiole length phenotypes of *dwe1* appeared partially recovered (Supplemental Fig. S2A). Moreover, the shorter hypocotyls of dark-grown *dwe1* plants were completely complemented by treatment with 0.5 μM BL (Supplemental Fig. S2, B and C). Together, these findings indicate that *dwe1* is likely impaired in BR biosynthesis.

DWE1 Mutation Confers Increased Resistance to Insect Herbivory and Pathogen Infection

Previous studies reveal that a mutation in BR biosynthesis partially restores JA sensitivity in the *coi1-2* mutant, a leaky mutant of the JA receptor, COI1, that exhibits partial fertility (Ren et al., 2009). Given that the *PDF1.2* genes were upregulated in *dwe1*, we investigated whether the mutation to *DWE1* alters plant responses to JA. Treatment with 50 μM MeJA inhibited primary root growth in wild-type seedlings, whereas *coi1-2* showed insensitivity to JA inhibition of root growth (Fig. 2A), as previously reported (Staswick et al., 1992; Xiao et al., 2004). Compared to the wild type, the roots of *dwe1*

seedlings showed enhanced sensitivity to MeJA treatment (Fig. 2A), as confirmed by calculating relative root length (Fig. 2B).

To further verify the effect of BR on the JA pathway, we crossed the *dwe1* mutant with *coi1-2* to generate the *dwe1 coi1* double mutant. When treated with 50 μM MeJA, the MeJA hypersensitivity of *dwe1* was rescued by the addition of the *coi1* mutation, as revealed by the greater root elongation of *dwe1 coi1* seedlings compared to the wild type and *dwe1* (Fig. 2, A and B).

JA is a major signaling molecule that regulates plant responses to insect herbivory and necrotrophic pathogen infection (Wasternack and Hause, 2013). To address whether DWE1 affects JA-mediated plant defense responses, we conducted insect feeding and pathogen inoculation assays on 4-week-old wild-type, *dwe1*, *dwe1 coi1*, and *coi1-2* plants using beet armyworm (*S. exigua*) and the fungus *B. cinerea*. Similar to previous findings (Howe and Jander, 2008; Hu et al., 2013), *coi1-2* was hypersensitive to both *S. exigua* feeding and *B. cinerea* infection compared to wild-type plants (Fig. 2, C and E), as confirmed by measuring larval weight and lesion size, respectively (Fig. 2, D and F). By contrast, compared to the wild type and *coi1-2*, *dwe1* was more resistant to *S. exigua* and *B. cinerea* (Fig. 2, C–F). Moreover, the *dwe1 coi1* double mutant showed partially restored

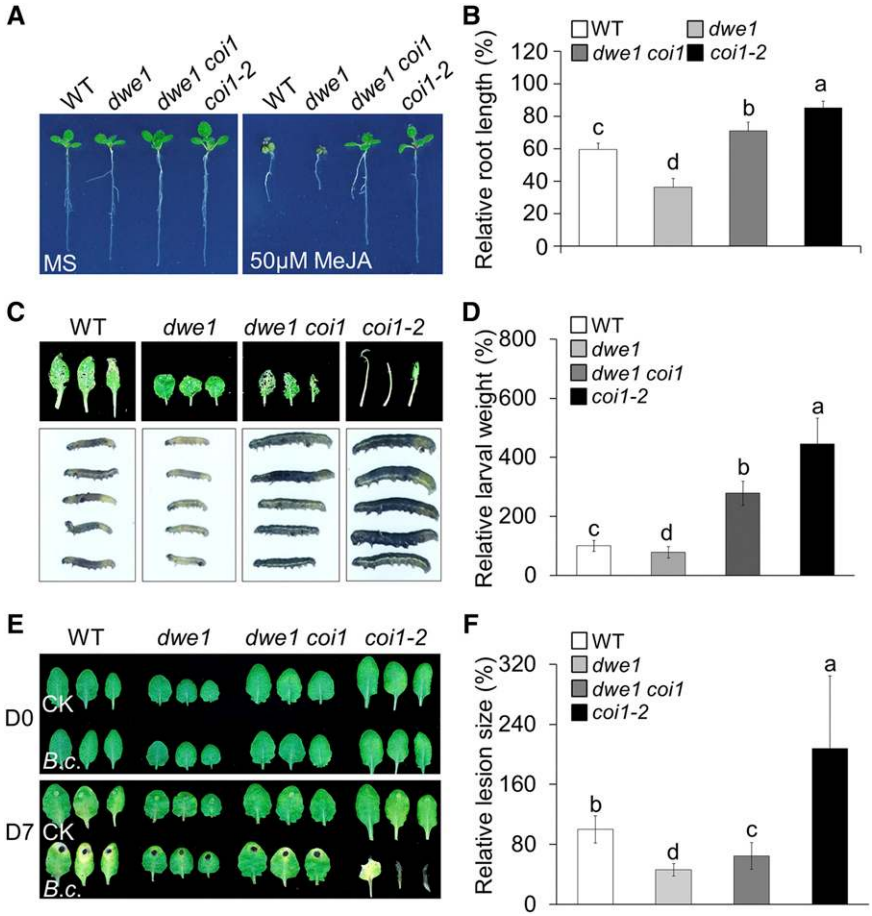

Figure 2. The *dwe1* mutant partially reduces the insensitivity of *coi1-2* to MeJA and suppresses the hypersensitivity of *coi1-2* to insect herbivory and pathogen infection. A and B, Root lengths (A) of 10-d-old wild-type (WT), *dwe1*, *dwe1 coi1*, and *coi1-2* seedlings grown on MS or MS medium containing 50 μM MeJA. Relative root elongation is expressed as a percentage of root elongation on MS medium. The experiments were biologically repeated three times with similar results. Error bars represent SD ($n > 20$ roots). Different letters indicate significant differences at $P < 0.05$ (one-way ANOVA with a Tukey HSD test). C, Phenotypes of leaves from 4-week-old wild-type, *dwe1*, *dwe1 coi1*, and *coi1-2* plants after 7 d of herbivory by *S. exigua*. Representative insects taken from the corresponding plants are shown below the rosette leaves. D, *S. exigua* larval weights for each genotype after 7 d feeding as shown in C is expressed as a percentage of wild-type. The experiments were biologically repeated three times with similar results. Error bars represent SD ($n > 30$ larvae). Different letters indicate significant differences at $P < 0.05$ (one-way ANOVA with a Tukey HSD test). E, Phenotypes of leaves from 4-week-old wild type, *dwe1*, *dwe1 coi1*, and *coi1-2* at 0 (D0) and 7 (D7) days after inoculation with *B. cinerea* (*B.c.*). The corresponding leaves inoculated with buffer without *B. cinerea* were treated as controls (CK). F, Statistics of lesion diameters for each genotype as shown in E is expressed as a percentage of wild type. The experiments were biologically repeated three times with similar results. Error bars represent SD ($n > 15$ leaves). Different letters indicate significant differences at $P < 0.05$ (one-way ANOVA with a Tukey HSD test).

susceptibility to *S. exigua* herbivory and significantly improved resistance to *B. cinerea* infection compared to the *coi1-2* single mutant (Fig. 2, C–F), suggesting that DWE1 may operate differentially in JA signaling to *S. exigua* and *B. cinerea* responses. However, even though JA sensitivity and resistance to insect herbivory and pathogen infection were partially restored in *coi1-2* by crossing with *dwe1*, the suppressed male fertility of *coi1-2* was not restored in the *dwe1 coi1* double mutant (Supplemental Fig. S2D).

dwe1 Is a Knockout Allele of *ROT3*

To isolate the genetic locus for the *dwe1* mutation, we produced an F2 mapping population by crossing *dwe1* (Col-0 background) with wild-type Landsberg *erecta* (L*er*) plants. Analysis of the segregation ratio in the *dwe1* × L*er* F2 population indicated that the semidwarf phenotype of the *dwe1* mutant is due to a single recessive mutation. Based on linkage analysis among molecular markers and the semidwarf phenotype of *dwe1* in dwarf F2 progeny, we localized *DWE1* to chromosome IV between two simple sequence-length polymorphism markers, A9791 (20 recombinants) and B18036 (five recombinants; Fig. 3A).

After fine mapping, we further narrowed down the location of the mutation to a 110-kb genomic region between markers A17120 (two recombinants) and B17230 (one recombinant), which contains two overlapping bacterial artificial chromosomes (F23E13 and AP22) and 33 candidate genes (Fig. 3A). By analyzing the mRNA levels of these candidate genes, we determined that *ROT3* (encoded by AT4G36380) is completely downregulated in *dwe1* versus the wild type (Fig. 3D). PCR analysis and sequencing of the PCR products localized the T-DNA insertion site at −182 bp on 5′-untranslated regions in *ROT3* (Fig. 3, B and C), where the insertion resulted in the null mutation of *ROT3* (Fig. 3D).

To validate the identity of *ROT3*, we performed a genetic complementation assay. We amplified the coding sequence (CDS) of *ROT3* from wild-type Col-0, cloned it into a construct where its expression was driven by the *35S* promoter, and introduced it into the *dwe1* mutant via *Agrobacterium tumefaciens*-mediated transformation. The dwarfism phenotypes and the shorter hypocotyls of dark-grown *dwe1* mutant were complemented by the introduction of *ROT3* (Supplemental Fig. S3). Moreover, two independent transgenic lines (*dwe1 35S::ROT3 #1* and *dwe1 35S::ROT3 #9*) exhibited levels of sensitivity to *S. exigua* and *B. cinerea* similar to those of the wild type (Fig. 3, E and F), confirming that the phenotypic changes in *dwe1* are due to the knockout of *ROT3*.

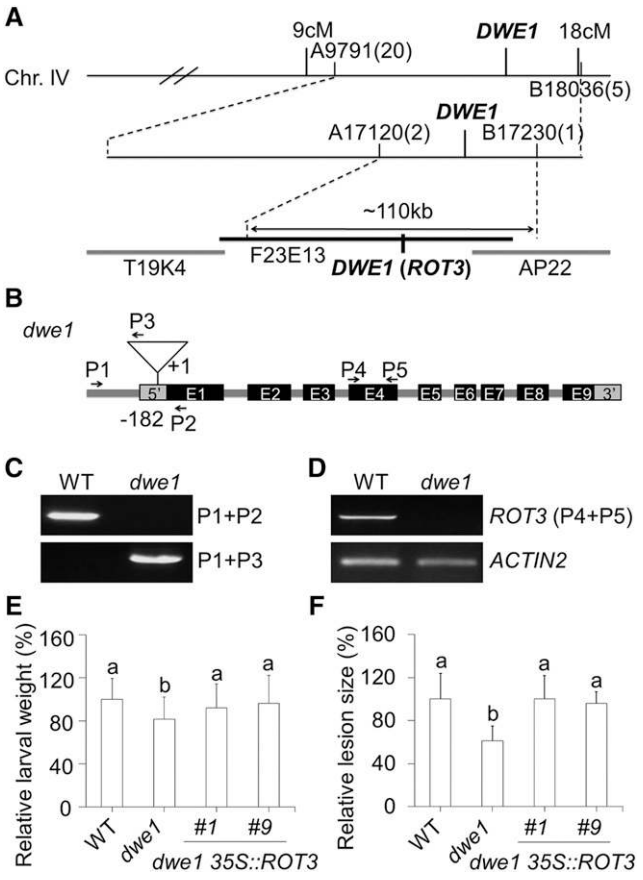

Figure 3. Map-based cloning and complementation test of *DWE1*. A, The *DWE1* locus is located on chromosome IV between markers A9791 (20 recombinants) and B18036 (five recombinants). The gene was further mapped to two bacterial artificial chromosomes (F23E13 and AP22) between the markers A17120 (two recombinants) and B17230 (one recombinant). cM, centimorgans; kb, kilobases. T19K4 is a BAC clone overlapped with F23E13. B, Diagram of the genomic region flanking the T-DNA insertion site in *dwe1*. The gray and black boxes indicate untranslated regions and exons, respectively. P1, P2, and P3 are primers used for PCR analysis. C, PCR analysis of the wild-type (WT) and *dwe1* showing the T-DNA insertion site at −182 bp on 5′-untranslated regions in *dwe1*. D, RT-PCR analysis showing presence of *ROT3* mRNA in wild-type and *dwe1* plants. E and F, Complementation of the *dwe1* mutation by *ROT3*. Four-week-old wild-type, *dwe1*, and two independent complemented transformants (*dwe1 35S::ROT3 #1*, and *#9*) were exposed to *S. exigua* and *B. cinerea*. Larval weights (E) and lesion diameters (F) at 7 d after treatment is expressed as a percentage of wild-type. The experiments were biologically repeated three times with similar results. Error bars represent SD ($n > 30$ larvae for *S. exigua* feeding, and $n > 15$ leaves for *B. cinerea* infection). Different letters indicate significant differences at $P < 0.05$ (one-way ANOVA with a Tukey HSD test).

BES1 Contributes to BR-Induced Suppression of Plant Defense Responses

BES1 and BZR1 are key transcription factors that function downstream of BR signal transduction by targeting numerous BR-responsive genes (Sun et al., 2010; Yu et al., 2011). Given that *dwe1* is deficient in the biosynthesis of BR, which antagonizes JA-mediated plant defense signaling, we reasoned that cross talk between BR and JA signaling might mediate the balance between plant growth and defense responses. To investigate this notion, we measured the transcript

levels of the JA-responsive genes *PDF1.2a*, *PDF1.2b*, and *VSP1* in wild-type plants and in the gain-of-function mutants *bes1-D* and *bzr1-1D* (Wang et al., 2002; Yin et al., 2002; Vilarrasa-Blasi et al., 2014) in the presence and absence of 100 μM MeJA. Compared to the mock control (treatment with water), all three genes were significantly upregulated in wild-type seedlings after 6 h of MeJA treatment (Fig. 4A). In contrast to wild-type seedlings, these genes were significantly downregulated in *bes1- D* under control conditions and after MeJA treatment, whereas *PDF1.2b* and *VSP1* were significantly upregulated in *bzr1-1D* (Fig. 4A) after MeJA treatment. Moreover, when we applied 200 nM BL together with MeJA, the MeJA-triggered induction of all three genes was suppressed in all three genotypes (Fig. 4A). These results suggest that BES1 is involved in BR-induced suppression of plant defense gene expression.

To further investigate the role of BES1 in JA-mediated defense against pathogen invasion, we exposed 4-week-old wild-type, *bes1- D*, loss-of-function mutant *bes1-2*, and *coi1-2* plants to *B. cinerea*. Compared to the wild type, the *bes1-D* mutant was more susceptible to *B. cinerea* inoculation, similar to *coi1-2* (Fig. 4B), as indicated by lesion size measurements (Fig. 4C). By contrast, compared to the wild type, *bes1-2* exhibited increased resistance to *B. cinerea*, as indicated by reduced lesion size (Fig. 4, B and C).

BES1 Regulates Plant Susceptibility to *B. cinerea* by Targeting the Downstream Terminators of *PDF1.2s*

To determine the molecular nature of BES1-mediated plant defense responses to a necrotrophic pathogen, we investigated whether BES1 directly associates with the promoters of *PDF1.2a* and *PDF1.2b*. BES1 binds to BRRE (CGTGTG and CGTGCG), E-box (CANNTG), and G-box (e.g. CACGTG) elements in the promoters of its target genes to activate or suppress their expression (Yin et al., 2005; Ye et al., 2012; Martínez et al., 2018). Bioinformatic analysis revealed several potential BES1-binding elements in the 5′ promoter regions of *PDF1.2a* and *PDF1.2b* (Fig. 5A). Using the *BES1-L-GFP* transgenic line (Jiang et al., 2015), we performed chromatin immunoprecipitation (ChIP)-qPCR to examine the interaction between BES1 and *PDF1.2a* or *PDF1.2b*. However, we did not detect an enrichment of BES1 in the 5′ promoter regions of *PDF1.2a* and *PDF1.2b* in *BES1-L-GFP* seedlings using anti-GFP antibodies (Fig. 5B).

Transcription factors frequently bind to the cis elements in the coding regions or downstream regions of terminators to regulate target gene expression (Yant et al., 2010; Franco-Zorrilla et al., 2014; Yan et al., 2014). We therefore analyzed the coding and downstream regions of *PDF1.2a* and *PDF1.2b* and identified several BES1-binding sites in these regions (Fig. 5A). ChIP-qPCR revealed strong enrichment of two BES1-bound DNA fragments from the 3′ downstream regions of *PDF1.2a* (P5 and P6) and *PDF1.2b* (P2 and P3; Fig. 5B). The *ACTIN2* (*ACT2*) promoter fragment, assessed as a control, did not show any detectable interactions with BES1 (Fig. 5B).

To further confirm the ChIP-qPCR data, we carried out an electrophoretic mobility shift assay (EMSA) to determine the in vitro interactions between BES1 and the P5/P6 and P2/P3 elements in *PDF1.2a* and *PDF1.2b*, respectively. We expressed recombinant His-BES1 protein in *Escherichia coli*. When purified His-BES1 protein

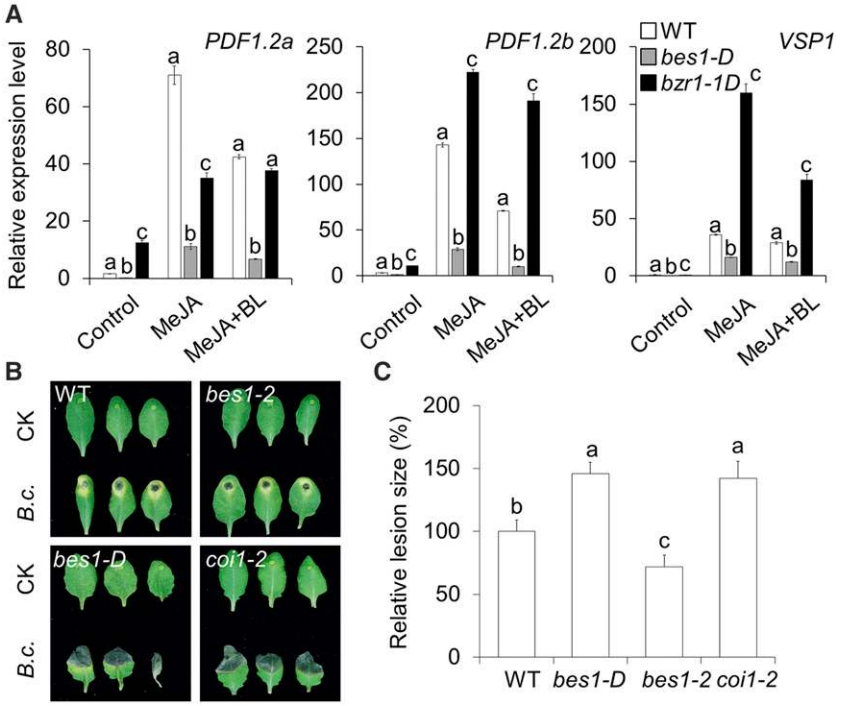

Figure 4. BES1 is essential for BR-mediated suppression of plant resistance to necrotrophic pathogen infection. A, RT-qPCR analysis of the JA-inducible genes *PDF1.2a*, *PDF1.2b*, and *VSP1* in 7-d-old wild-type (WT), *bes1-D*, and *bzr1-1D* plants treated with water (control), 100 μM MeJA (MeJA), or 100 μM MeJA with 200 nM BL (MeJA + BL) for 6 h. Transcripts were normalized to levels of *ACTIN2*. The experiments were biologically repeated three times with similar results. Error bars represent SD ($n = 3$ technical replicates). Different letters indicate significant differences within the same treatment at $P < 0.05$ (one-way ANOVA with a Tukey HSD test). B, Phenotypes of leaves from 4-week-old plants of wild-type, *bes1-D*, *bes1-2*, and *coi1-2* plants at 5 d after inoculation with *B. cinerea* (*B.c.*) or buffer without *B. cinerea* (CK). C, Statistics of mean lesion diameter for the genotypes shown in B is expressed as a percentage of wild-type. The experiments were biologically repeated three times with similar results. Error bars represent SD ($n >$ 15 leaves). Different letters indicate significant differences at $P < 0.05$ (one-way ANOVA with a Tukey HSD test).

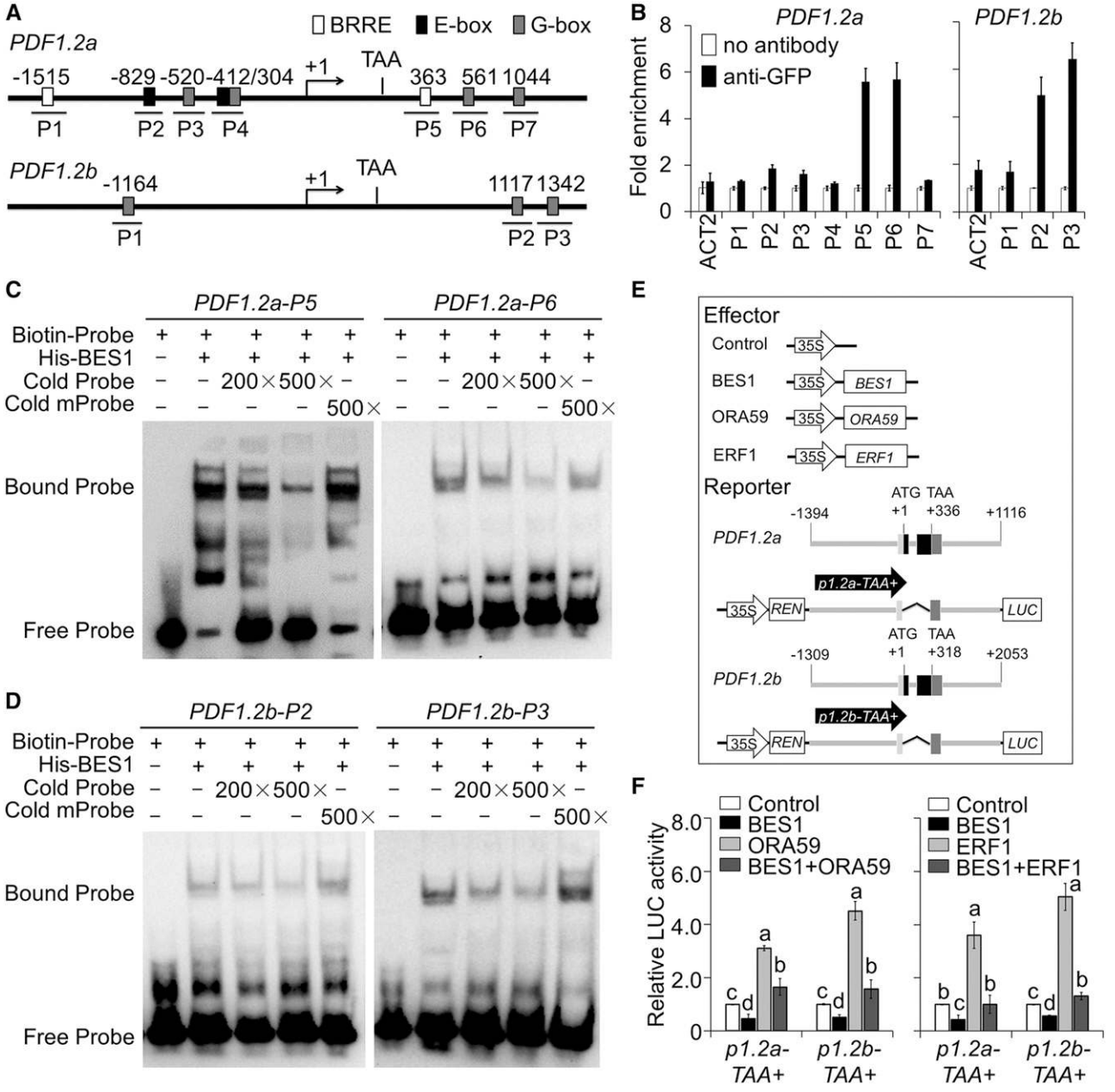

Figure 5. BES1 interacts with the downstream terminator regions of *PDF1.2a* and *PDF1.2b* and suppresses their transcriptional activities. A, Schematic diagrams indicating the locations of putative BES1 binding sites (BRRE, E-box, and G-box elements) in the promoter, coding, and downstream terminator regions of *PDF1.2a* (P1 to P7) and *PDF1.2b* (P1 to P3) genomic sequences. Numbers indicate the nucleotide positions relative to their corresponding translational start site (ATG), which is shown as +1 with arrows. B, ChIP-qPCR assays showing the interactions between BES1 and BRRE/G-box elements at the terminator regions of *PDF1.2a* and *PDF1.2b*. The assays were performed using 12-d-old *BES1-L-GFP* transgenic plants treated with 1 μM BL for 2 h. Primers used for ChIP-qPCR were specific to the regions containing the BRRE, E-box, or G-box motif sites shown in A. *ACT2* was used as a negative control. The qPCR results were normalized against the input samples. The experiments were biologically repeated three times with similar results. Error bars represent SD ($n = 3$ technical replicates). C and D, EMSA assays detecting the binding of BES1 to the downstream terminators of *PDF1.2a* (C) and *PDF1.2b* (D). E, Schematic diagrams of effector and reporter constructs used in the transient LUC assays. The *35SPPDK* promoter driving *BES1* (*35S::BES1*), *ORA59* (*35S::ORA59*), and *ERF1* (*35S::ERF1*) were used as effectors. The empty vector was used as a control. The gene structures of *PDF1.2a* and *PDF1.2b* are shown in the bottom. Exons are shown as black boxes; promoter, introns, and downstream regions of terminator are indicated as lines; and 5′ and 3′ untranslated regions are shown as light gray and dark gray boxes, respectively.The dual-luciferase reporter constructs consist of *35S* driving the *Renilla luciferase* (*REN*) reporter gene (expressed for internal normalization) and the promoter fragment linking downstream regions of *PDF1.2a* (*p1.2a-TAA+*) and *PDF1.2b* (*p1.2b-TAA+*) terminators of driving the

was incubated with the *PDF1.2a-P5*, *PDF1.2a-P6*, *PDF1.2b-P2*, and *PDF1.2b-P3* probes in the absence or presence of cold probe competitors, it bound specifically to the P5 and P6 fragments of *PDF1.2a* and the P2 and P3 fragments of *PDF1.2b*, whereas no binding was detected in a control lacking His-BES1 (Fig. 5, C and D). Moreover, unlabeled probes (cold probe) competed with *PDF1.2a-P5*, *PDF1.2a*-P6, *PDF1.2b-P2*, and *PDF1.2b-P3* for binding to His-BES1 in a dose-dependent manner (Fig. 5, C and D, lanes 3 and 4). By contrast, unlabeled mutated probe (cold mProbe) failed to compete with these fragments (Fig. 5, C and D, lane 5). These results, together with in vivo ChIP data, suggest that *PDF1.2a* and *PDF1.2b* are direct target genes of BES1.

To assess the effects of BES1 on the transcriptional regulation of *PDF1.2a* and *PDF1.2b*, we conducted a dual-luciferase (LUC) reporter assay in Arabidopsis protoplasts. We fused the 5′ promoter, coding linked 3′ downstream, and 3′ downstream regions of *PDF1.2a* and *PDF1.2b* with *LUC* to generate the *p1.2a-LUC*, *1.2a ATG+-LUC*, *1.2a TAA+-LUC*, *p1.2b-LUC*, *1.2b ATG+-LUC*, and *1.2b TAA+-LUC* reporters (Supplemental Fig. S4, A and B). In addition, we constructed an effector using the *35SPPDK* promoter to drive the expression of BES1 (Supplemental Fig. S4). When we transiently expressed the plasmids in Arabidopsis protoplasts, the activities of *1.2a TAA+-LUC* and *1.2b TAA+-LUC*, but not the other reporters, were significantly suppressed by the presence of BES1 (Supplemental Fig. S4), indicating that BES1 transcriptionally suppresses the expression of *PDF1.2a* and *PDF1.2b*.

ORA59 and ERF1 are key AP2/ERF transcription factors that activate the transcription of *PDF1.2a* and *PDF1.2b* by directly binding to their promoters (Pré et al., 2008; Zarei et al., 2011). We therefore examined whether BES1 competes with ORA59 or ERF1 for the transcriptional regulation of their common target genes. Coexpression of BES1 with ORA59 or ERF1 (Fig. 5, E and F) significantly attenuated the activation of both *p1.2a-TAA+-LUC* and *p1.2b-TAA+-LUC* (Fig. 5F). The *Luciferase* genes were driven by the *PDF1.2a/b* promoter regions and linked to the downstream regions of *PDF1.2a/b* terminators.

To uncover the genetic link between the susceptibility of *bes1-D* to biotic stress and the transcriptional regulation of *PDF1.2a*, we generated two stable transgenic lines overexpressing *PDF1.2a* (named *PDF1.2a-OE1* and *PDF1.2a-OE2*; Supplemental Fig. S5A) and crossed them with *bes1- D* to obtain *PDF1.2a-OE bes1-D1* and *PDF1.2a-OE bes1-D2*. As expected, *PDF1.2a-OE1* and *PDF1.2a-OE2* displayed enhanced resistance to *B. cinerea* inoculation (Supplemental Fig. S5B). Compared to the hypersensitivity of *bes1-D*, the responses of *PDF1.2a-OE bes1-D1* and *PDF1.2a-OE bes1-D2* to *B. cinerea* resembled those of the *PDF1.2a-OEs* (Supplemental Fig. S5B). Together, our findings indicate that the BES1-*PDF1.2a* interaction contributes to defense response against necrotrophic pathogen invasion.

BR Antagonizes Insect Herbivory-Induced Indolic GS Biosynthesis

To investigate the function of BES1 in JA-mediated defense against insect herbivory, 4-week-old wild-type, *bes1-D*, *bes1-2*, and *coi1-2* plants were exposed to *S. exigua*. Compared to the wild type, the *bes1-D* mutant showed increased sensitivity to *S. exigua* feeding similar to *coi1-2* (Fig. 6A), as revealed by measuring larval weight (Fig. 6B). By contrast, compared to the wild type, *bes1-2* exhibited enhanced resistance to *S. exigua*, as indicated by reduced larval weights (Fig. 6, A and B). The sensitivities of *PDF1.2a-OE1* and *PDF1.2a-OE2* to *S. exigua* feeding appeared similar to that of wild type (Supplemental Fig. S5C). Further, overexpression of *PDF1.2a* had little effect on the susceptibility of *bes1-D* to *S. exigua* herbivory (Supplemental Fig. S5C).

GSs are nitrogen- and sulfur-containing secondary metabolites produced in response to insect herbivory. These compounds act downstream of JA signaling to promote insect resistance (Schweizer et al., 2013). We therefore reasoned that BES1 may act in plant response to insect herbivory by regulating GS biosynthesis. To test this hypothesis, we measured the level of various GSs, including the indolic GSs indol-3-ylmethyl-GS (I3M) and 1-methoxyindol-3-ylmethyl-GS (1-MOI3M) and the aliphatic GSs 4-methylsulfinylbutyl-GS (4-MOSB), 5-methylsulfinylpentyl-GS (5-MSOP), 4-methylthiobutyl-GS (4-MTB), and 8-methylsulfinyloctyl-GS (8-MSOO) in wild-type, *dwe1*, *coi1-2*, *bes1-2*, and *bes1-D* rosettes after 3 d of *S. exigua* feeding. The accumulation of indolic GS species (I3M and 1-MOI3M) in response to *S. exigua* feeding was significantly elevated in *dwe1* and *bes1-2* but significantly reduced in *bes1-D* compared to the wild type (Fig. 6C; Supplemental Fig. S6). By contrast, the levels of aliphatic GSs including 4-MOSB, 5-MSOP, and 8-MSOO were not significantly altered in *dwe1*, although the levels of 4-MOSB, 5-MSOP, and 8-MSOO increased in *bes1-2*, and 4-MOSB, 4-MTB decreased in *bes1-D* in response to *S. exigua* feeding (Fig. 6C; Supplemental Fig. S6). Moreover, the levels of aliphatic GSs including 4-MOSB, 5-MSOP, 4-MTB, and 8-MSOO were significantly reduced in *coi1-2* (Supplemental Fig. S6). These findings indicate that BES1 antagonizes insect-herbivory-induced indolic GS biosynthesis in Arabidopsis.

Figure 5. (*Continued.*)
firefly LUC reporter gene. F, Dual-luciferase (LUC) reporter assays showing the suppression of *PDF1.2a* and *PDF1.2b* transcriptions by BES1. Effects of BES1 on ORA59- and ERF1-activated transcription of *PDF1.2a* and *PDF1.2b* in wild-type (Col-0) protoplasts. The experiments were biologically repeated three times with similar results. Error bars represent SD ($n = 3$ technical replicates). Different letters indicate significant differences at $P < 0.05$ (one-way ANOVA with a Tukey HSD test).

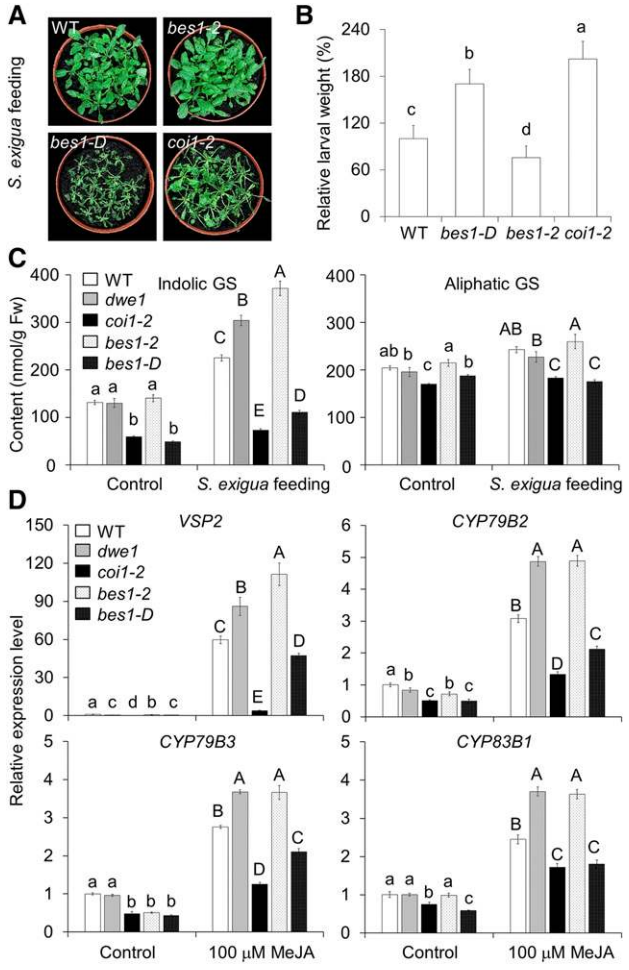

Figure 6. BR antagonizes JA-dependent indolic GS synthesis in response to *S. exigua* herbivory. A, Phenotypes of 4-week-old plants of wild-type (WT), *bes1-D*, and *bes1-2* after 7 d of herbivory by *S. exigua*. The *coi1-2* mutant was used as a positive control. B, *S. exigua* larval weights after 7 d of feeding for the genotypes shown in A are expressed as a percentage of wild type. The experiments were biologically repeated three times with similar results. Error bars represent SD ($n > 30$ larvae). Different letters indicate significant differences at $P < 0.05$ (one-way ANOVA with a Tukey HSD test). C, Ultra-HPLC/quadrupole time-of-flight measurements showing the levels of indolic GS and aliphatic GS in wild-type, *dwe1*, *coi1-2*, *bes1-2*, and *bes1-D* untreated plants (control) and in plants treated with *S. exigua* for 3 d. The experiments were biologically repeated twice with similar results. Error bars represent SD ($n = 4$ technical replicates). Fw, fresh weight. Different letters within each treatment indicate significant differences at $P < 0.05$ (one-way ANOVA with a Tukey HSD test); capital letters compare with each other, and lowercase letters compare with each other. D, RT-qPCR showing the expression levels of the indolic GS biosynthesis genes (*CYP79B2*, *CYP79B3*, and *CYP83B1*) in wild-type, *dwe1*, *coi1-2*, *bes1-2*, and *bes1-D* plants in response to water (control) or MeJA (100 μM MeJA) treatment for 12 h. The JA-inducible maker gene *VSP2* was used as a positive control. For each genotype, transcript levels relative to wild-type control were normalized to that of *ACTIN2*. The experiments were biologically repeated three times with similar results. Error bars represent SD ($n = 3$ technical replicates). Different letters within each treatment indicate significant differences at $P < 0.05$ (one-way ANOVA with a Tukey HSD test); capital letters compare with each other, and lowercase letters compare with each other.

To further verify the association between BES1-mediated suppression of indolic GS biosynthesis and the JA signaling pathway, we treated wild-type, *dwe1*, *coi1-2*, *bes1-2*, and *bes1-D* seedlings with exogenous 100 μM MeJA and measured the expression levels of three indolic GS synthesis genes (*CYP79B2*, *CYP79B3*, and *CYP83B1*). The JA-induced expression levels of these genes were significantly higher in *dwe1* and *bes1-2* but significantly lower in *bes1-D* than in the wild type (Fig. 6D). By contrast, the elevated expression of these genes in response to MeJA treatment were abolished in *coi1-2* (Fig. 6D). As a control, the expression of *VSP2* was significantly induced the wild-type plants upon MeJA treatment but was down-regulated in the *coi1-2* and *bes1-1D* mutants and up-regulated in the *dwe1* and *bes1-2* mutants (Fig. 6D). These results indicate that BES1 suppresses the JA-induced indolic GS biosynthetic gene expression.

BES1 Interacts with MYB Transcription Factors Essential for GS Biosynthesis

In Arabidopsis, six MYB transcription factors (MYB34, MYB51, MYB122, MYB28, MYB29, and MYB76) are master regulators of genes involved in GS biosynthesis (Gigolashvili et al., 2007, 2008; Frerigmann and Gigolashvili, 2014). Despite the fact that investigations revealed the inhibition of GS biosynthesis by BRs, little is known about the molecular mechanism(s) by which BRs regulate GS biosynthesis. Previous studies speculate that BES1 and BZR1 might inhibit the GS synthesis by regulating either the GS biosynthesis genes or the MYB transcription factors (Chen and Andreasson, 2001; Guo et al., 2013). We therefore reasoned that BES1 regulates plant sensitivity to insect herbivory by interacting with these MYBs to attenuate GS biosynthesis. To test this hypothesis, we generated constructs expressing *MYB34-*, *MYB51-*, *MYB122-*, *MYB28-*, *MYB29-*, and *MYB76-FLAG*, as well as *BES1-HA* fusion proteins, for coimmunoprecipitation (CoIP) assays. When *BES1-HA* and *MYBs-FLAG* were transiently coexpressed in wild-type Arabidopsis leaf protoplasts, most MYBs were immunoprecipitated by BES1 (Fig. 7A).

To further validate the association of the MYBs with BES1, we performed bimolecular fluorescence complementation (BiFC) analysis using Arabidopsis proteins fused with split yellow fluorescent protein (YFP). We transiently coexpressed *MYB34-*, *MYB51-*, *MYB122-*, *MYB28-*, *MYB29-*, or *MYB76-nYFP* with *BES1-cYFP* in protoplasts for 16 h and then examined them by confocal microscopy. The nuclear ARF4-RFP fusion protein (Sun et al., 2019) was coexpressed in all experiments as a marker. We detected YFP signals in the nuclei for all MYB-nYFP and BES1-cYFP combinations (Fig. 7B). By contrast, coexpression of the nYFP empty vector with BES1-cYFP or the cYFP empty vector with MYB-nYFP failed to reconstitute an intact YFP signal in Arabidopsis leaf protoplasts (Fig. 7B; Supplemental Fig. S7A).

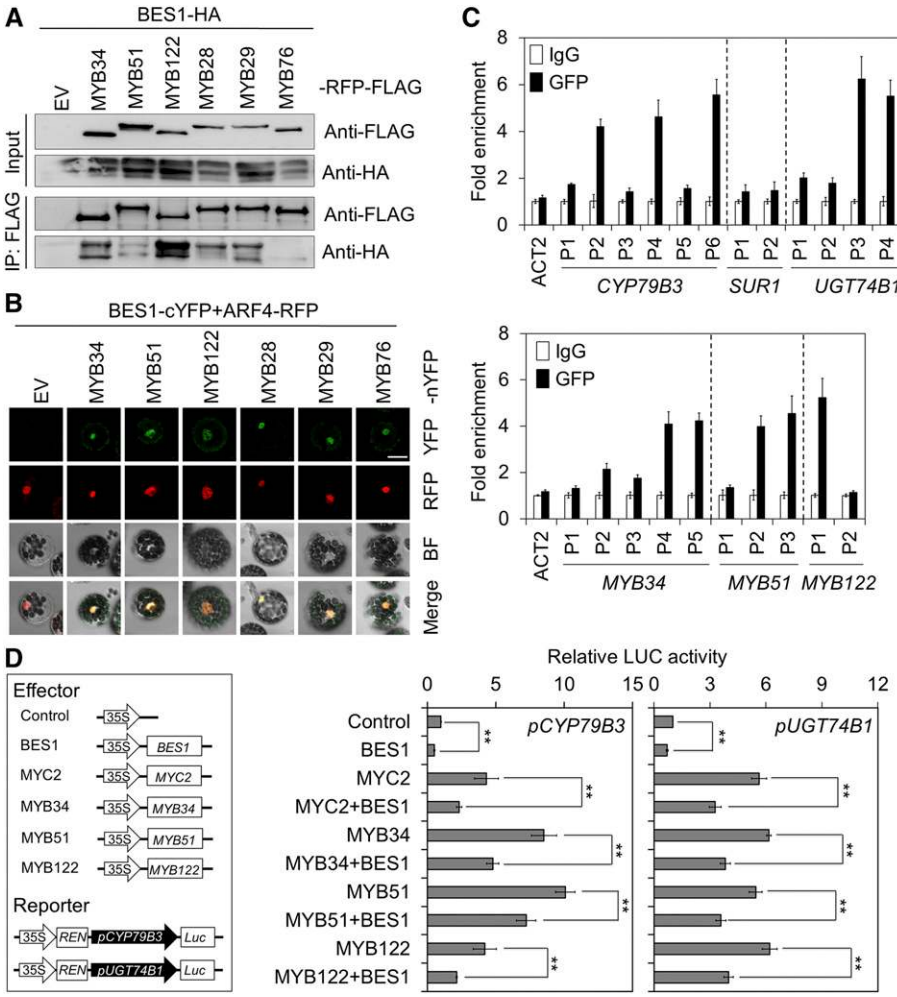

Figure 7. BES1 interacts with MYB transcription factors to alleviate the MYB-activated transcription of genes involved in GS biosynthesis. A, In-vivo CoIP assay showing the physical interactions between BES1 and MYB34, MYB51, MYB122, MYB28, and MYB29. HA-tagged BES1 (*BES1-HA*) was coexpressed with FLAG-tagged MYBs (*MYB34-*, *MYB51-*, *MYB122-*, *MYB28-*, *MYB29-*, and *MYB76-FLAG*) in wild-type (WT; Col-0) Arabidopsis protoplasts and immunoprecipitated by FLAG affinity magnetic beads. EV, empty vector. B, BiFC assay showing the interaction between BES1 and MYBs proteins. The split nYFP and cYFP fusions *BES1-cYFP* and *MYBs-nYFP* (*MYB34-*, *MYB51-*, *MYB122-*, *MYB28-*, *MYB29-*, and *MYB76-nYFP*) were coexpressed in wild-type protoplasts for 16 h, followed by confocal microscopy. The *ARF4-RFP* vector was coexpressed as a nuclear localization marker. BF, Bright field. Bar = 10 μm. C, ChIP-qPCR analysis of the in vivo binding of *BES1-L-GFP* to the promoters of *CYP79B3* (P1 to P6), *SUR1* (P1 and P2), *UGT74B1* (P1 to P5), *MYB34* (P1 to P5), *MYB51* (P1 to P3), and *MYB122* (P1 and P2). Primers used for ChIP-qPCR were specific to the regions containing the BRRE, E-box, or G-box elements. *ACT2* was used as a negative control. The qPCR results were normalized against the input samples. The dashed lines separate the results from the different genes. The experiments were biologically repeated three times with similar results. Error bars represent SD ($n = 3$ technical replicates). D, Dual-luciferase (LUC) reporter assays showing the suppression of *CYP79B3* and *UGT74B1* transcription by BES1. Left, Schematic diagrams of effector and reporter constructs used in the transient LUC assays. *35SPPDK* promoter driving *BES1*, *MYC2*, *MYB34*, *MYB51*, and *MYB122* were used as an effector. The empty vector was used as a control. The dual-luciferase reporter constructs consist of 35S driving *Renilla luciferase* (*REN*) reporter gene for internal normalization, and the promoters of *CYP79B3* and *UGT74B1* driving *firefly LUC* reporter gene. Right, Effects of BES1 on the MYC2-, MYB34-, MYB51-, MYB122-activated transcription of *CYP79B3* and *UGT74B1* in wild-type protoplasts. The experiments were biologically repeated three times with similar results. Error bars represent SD ($n = 3$ technical replicates). Asterisks denote Student's *t* test significance between indicated samples (**$P < 0.01$).

These results suggest that BES1 physically interacts with all six MYB transcription factors in vivo.

Bioinformatic analysis identified several BES1-binding cis elements, including BRRE, E-box (CANNTG), and G-box motifs, in the promoters of various GS biosynthetic genes, such as *CYP79F1*, *CYP83A1*, *CYP79B3*, *UGT74B1*, and *SUR1*, as well as all six *MYB* genes (Supplemental Fig. S7B). We performed ChIP-qPCR assays to determine whether BES1 associates with these cis elements in vivo. Consistent with the results of GS measurements

and RT-qPCR (Fig. 6, C and D), BES1 bound to the promoters of indole-GS synthetic genes *CYP79B3* (P2, P4, and P6) and *UGT74B1* (P3 and P4), but not to *SUR1* or the aliphatic-GS genes *CYP79F1* or *CYP83A1* (Fig. 7C; Supplemental Fig. S7C). Moreover, BES1 bound directly to the promoters of the MYB genes *MYB34* (P4 and P5), *MYB51* (P2 and P3), and *MYB122* (P1; Fig. 7C), which encode transcription factors that specifically regulate indole-GS genes. However, we did not detect interactions between BES1 and the aliphatic GS-related *MYB* genes, except for *MYB76* (Supplemental Fig. S7C).

To further explore the role of BES1 in regulating GS biosynthesis, we cloned the promoter sequences of various GS-related genes and fused them to the *LUC* reporter. The presence of BES1 dramatically suppressed LUC activity driven by the *CYP79B3*, *UGT74B1*, *MYB34*, *MYB51*, *MYB76*, and *MYB122* promoters (Supplemental Fig. S8). Consistent with the ChIP-qPCR results, BES1 had little effect on the activities of the *pCYP79F1-*, *pCYP83A1-*, *pSUR1-*, *pMYB28-*, and *pMYB29-LUC* reporters (Supplemental Fig. S8).

MYC2 is a core transcription factor involved in JA signaling that activates GS biosynthesis by interacting with all known GS-related MYB transcription factors (Schweizer et al., 2013). To investigate a potential link between the BES1-mediated suppression of GS biosynthetic gene expression and MYC2-/indolic GS-related MYBs-mediated GS activation, we coexpressed BES1 with MYC2, MYB34, MYB51, or MYB122 and measured the effects on *pCYP79B3-LUC* and *pUGT74B1-LUC* activity. Whereas the expression of *pCYP79B3-LUC* and *pUGT74B1-LUC* was strongly activated in the presence of MYC2, MYB34, MYB51, or MYB122, it was significantly attenuated in the presence of BES1 (Fig. 7D). These results indicated that BES1 negatively regulates the transcriptional activities of MYC2 and GS-related MYBs to modulate the expression of indolic GS biosynthesis genes.

DISCUSSION

BRs are growth-promoting phytohormones that are thought to play a negative role in plant defense responses, which likely represent a key mechanism that fine tunes the tradeoff between plant growth and defense responses upon pathogen infection and insect herbivory (Albrecht et al., 2012; Belkhadir et al., 2012). However, although the physiological roles of BRs in responses to various biotic factors have been well studied, direct molecular evidence linking BRs to defense signaling has been lacking.

Here, we provided several lines of evidence supporting the roles of BRs in plant responses to a necrotrophic pathogen and insect attack. Specifically, we hypothesized that BES1 antagonizes JA-induced plant defense signaling by differentially suppressing the expression of defensin and GS biosynthesis genes. First, using genetic screens, we determined that the *dwe1* mutation, which leads to a semidwarf phenotype resembling that of BR-deficient mutants (Fig. 1), significantly suppressed the MeJA insensitivity and biotic stress susceptibility of the JA receptor *coi1* mutant (Fig. 2). Genetic mapping and complementation tests showed that *dwe1* is a knockout allele of *ROT3* (Fig. 3; Supplemental Fig. S3), encoding a BR C-23 hydroxylase essential for BR biosynthesis (Ohnishi et al., 2006). Second, the gain-of-function *bes1-D* mutant showed significantly reduced transcript levels of the JA-responsive genes *PDF1.2a* and *PDF1.2b* and was extremely susceptible to insect herbivory and pathogen invasion (Figs. 4 and 6). Third, biochemical analysis revealed that BES1 directly targeted the downstream terminator regions of *PDF1.2a* and *PDF1.2b* to attenuate their necrotrophic pathogen-induced transcriptional activities that are induced by ORA59 and ERF1 (Fig. 5). By contrast, BES1 physically interacts with indolic GS-related MYB transcription factors (MYB34, MYB51, and MYB122) and regulates the expression of indole-GS biosynthetic genes (*CYP79B3* and *UGT74B1*), leading to significant reductions in indole GS (I3M and 1-MOI3M) levels in *bes1-D* in the absence and presence of herbivory by *S. exigua* (Figs. 6 and 7; Supplemental Figs. S6–S8). Thus, our findings demonstrate that BES1 is a key transcription factor that antagonizes JA-activated plant defense responses by directly suppressing defensin and GS biosynthesis gene expression in Arabidopsis.

Plants have evolved sophisticated regulatory networks to help them cope with biotic and abiotic stress. During the past few decades, the specific roles of individual hormones in plant responses to various stresses have been well documented. However, the roles of the antagonistic and synergistic interactions of phytohormones in fine-tuning plant growth and defense responses require further investigation (Robert-Seilaniantz et al., 2011). Our findings suggest that the *DWE1/ROT3* knockout mutation partially reduces the insensitivity of *coi1-2* to MeJA, partially restores resistance to *S. exigua*, but fully suppresses the hypersensitivity of *coi1-2* to necrotrophic pathogen, indicating that DWE1 may operate differentially with JA signaling to *S. exigua* and *B. cinerea* responses. In particular, BES1 contributes to *B. cinerea* response by directly targeting *PDF1.2a* and *PDF1.2b* genes and suppressing their expression (Fig. 5), which may function in a COI1-independent manner. Involvement of BES1 in *S. exigua* response likely functions through interacting with the MYC2/MYB34/51/122 transcription complex and interfering with the transcription of GS biosynthesis genes (Figs. 6 and 7), which partially relies on a functional COI1 protein. These results reveal the different mechanisms of BES1 in modulation of JA-mediated responses to *S. exigua* herbivory and *B. cinerea* infection.

In particular, the *dwe1* mutant is an appropriate tool for investigating the role of the JA-BR interaction in mediating the plant growth-defense tradeoff. Indeed, MeJA treatment of wild-type seedlings significantly upregulated *PDF1.2a*, *PDF1.2b*, and *VSP1*; these JA-response genes are essential for plant defense responses (Pieterse et al., 2012). Treatment with a mixture

of MeJA and BL significantly decreased this response (Fig. 4A). These findings indicate that BR can suppress the JA-mediated plant defense to pathogen infection and insect herbivory. This is consistent with previous work indicating an antagonistic cross talk between BR and JA during plant growth and development (Ren et al., 2009; Huang et al., 2010; Peng et al., 2011; Gan et al., 2015). In particular, BR negatively regulates JA signaling and JA-inhibited root growth. By contrast, impairment of BR synthesis in the *dwarf4* (*dwf4*) mutant attenuates the negative effects of BR on JA-mediated root growth inhibition (Ren et al., 2009). Moreover, several studies imply that this antagonistic relationship between BR and JA likely functions in plant responses to herbivores (Campos et al., 2009; Yang et al., 2011; Miyaji et al., 2014). Our findings further extend this concept, highlighting the significance and molecular mechanisms of the JA-BR interaction in modulating plant immune responses.

Defensins are small, highly basic, Cys-rich peptides found in all living organisms, from microorganisms to plants and animals (Thomma et al., 2002). Most defensins show differential antimicrobial activities and are regarded as a primordial defense system against various pathogens. Arabidopsis contains 13 defensin genes, including three *PDF1.2* genes (*PDF1.2a*, *PDF1.2b*, and *PDF1.2c*) that are transcriptionally induced by pathogen exposure and JA and/or ET application (Thomma et al., 2002; Pieterse et al., 2012). Both JA and ET function in plant responses to necrotrophic pathogens (Pieterse et al., 2012). The ERF1 and ORA59 transcription factors in the JA and ET signaling pathways are activated upon infection by necrotrophic pathogens, which in turn activates *PDF1.2s* by ERF1 and ORA59 directly binding to their promoters (Zarei et al., 2011; Pieterse et al., 2012). Our data suggest that, in a mechanism analogous to the JA and ET signaling pathways, BES1 in the BR signaling pathway contributes to the negative modulation of plant resistance to the necrotrophic pathogen *B. cinerea* and the expression of *PDF1.2* genes (Fig. 4, A and B). However, BES1 associated with the G-box elements in the terminator regions, but not the promoters, of both *PDF1.2a* and *PDF1.2b* (Fig. 5, A and B), suggesting that BES1 antagonizes the ERF1/ORA59-induced transcription of *PDF1.2s* by binding to different G-box elements. The association of a transcription factor to the terminator region of target gene is likely a frequently occurring pattern in the regulation of target gene expression in plant cells (Yant et al., 2010; Franco-Zorrilla et al., 2014; Yan et al., 2014).

GSs are a class of nitrogen- and sulfur-containing secondary metabolites that confer plant resistance against insect herbivores (Bednarek et al., 2009; Clay et al., 2009). JA regulates, in conjunction with MYC2 and the GS-related MYBs (MYB28, MYB29, MYB76, MYB34, MYB51, and MYB122), GS production upon herbivore feeding (Zhou and Memelink, 2016). Among these MYBs, MYB34, MYB51, and MYB122 are responsible for indolic-GS biosynthesis and are synergistically activated by JA, ET, SA, and ABA (Frerigmann and Gigolashvili, 2014). These hormones promote GS biosynthesis, but BR suppresses GS accumulation in response to chewing insects (Guo et al., 2013).

We determined that upon herbivory, BES1 suppresses the transcriptional roles of MYC2 and GS-related MYBs in the activation of indolic GS-biosynthetic genes (Figs. 6D and 7). Furthermore, BES1 physically interacts with the indolic GS-associated transcription factors MYB34, MYB51, and MYB122 (Fig. 7, A and B). It is therefore possible that BES1 functions at multiple levels to regulate indolic GS biosynthesis during the balancing of BR-JA interactions. It is likely that JA- and insect herbivory-triggered indolic GS biosynthesis is tightly controlled by both positive JA signaling (through the MYC2/3/4/5-MYB34/51/122 module) and negative BR signaling (through the BES1-MYB34/51/122 module), the balance of which is a key factor determining plant susceptibility to insects. Our results also showed an opposite expression pattern of *bzr1-1D* in response to JA and BR application (Fig. 4A). In Arabidopsis, the *bzr1-1D* mutant shows dwarfism phenotypes resembling those of BR deficient mutants, which is distinct from *bes1-D* (Wang et al., 2002; Yin et al., 2002; He et al., 2005). Moreover, despite the high sequence identity (88%) between BZR1 and BES1 proteins, they can interact with different cofactors to regulate different plant responses (Li and Deng, 2005). Thus, it is conceivable that BZR1 may play a role distinct from that of BES1 in plant defense responses. Additional investigations of the mechanism by which BZR1 regulates downstream defense genes will further enrich our understanding of JA-BR cross talk.

Many BES1/BZR1 target genes have already been identified in plants (Sun et al., 2010; Guo et al., 2013). BES1 binds to the BRRE (CGTGT/CG), E-box (CANNTG), and G-box (e.g. CACGTG) elements of BR-activated genes, whereas BZR1 binds to the BRRE (CGTGT/CG) sequences and G-box (e.g. CACGTG) elements of BR-repressed genes (He et al., 2005; Yin et al., 2005; Sun et al., 2010; Yu et al., 2011; Martínez et al., 2018). In agreement with these findings, our data suggest that BES1 inhibits the transcription of indole-GS biosynthetic genes (*CYP79B3* and *UGT74B1*) by directly interacting with their G-box and BRRE elements (Fig. 7, C and D; Supplemental Figs. S7B and S8). Similarly, MYCs interact with the G-box and G-box variants of JA-responsive genes (Fernández-Calvo et al., 2011). In fact, ChIP-qPCR analysis in our study showed that BES1 bound to the G-box sites of *CYP79B3* and *UGT74B1* promoter regions, which are similar to that of MYC2 (Schweizer et al., 2013; Fig. 7C; Supplemental Fig. S7B). Moreover, dual-LUC reporter assays confirmed that BES1 attenuated the MYC2-activated expression of *CYP79B3* and *UGT74B1* (Fig. 7D). Based on these findings, it is likely that BES1 competes with MYCs for binding to G-box motifs in the regulation of JA-responsive genes. Increasing evidence suggests that BES1 physically interacts with other transcription factors, such as BES1-INTERACTING MYC-LIKE1 (BIM1) and MYB30, to induce BR-responsive gene

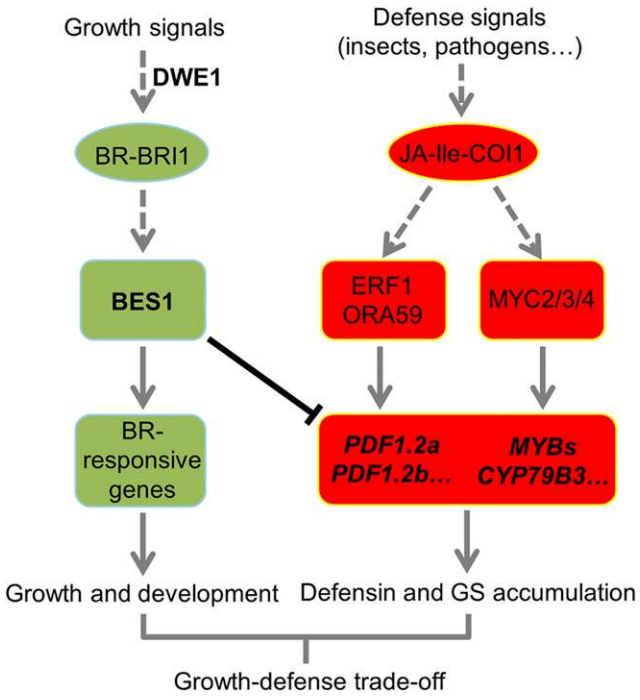

Figure 8. A working model showing the role of BES1 in fine-tuning plant growth-defense tradeoffs by suppressing JA-mediated defensin and glucosinolate biosynthesis. Plant growth signals trigger the expression of genes, including *DWE1*, to induce brassinosteroid (BR) synthesis. BR binds to the cell-surface receptor kinase BRI1 to activate BR signal transduction by sequential transphosphorylation events. The dephosphorylated transcription factor BES1 translocates into the nucleus, leading to the expression of BR-responsive genes and promotion of plant growth and development. By contrast, insect attack and pathogen infection induce the accumulation of JAs. The active form of JA, JA-Ile, is perceived by the COI1 receptor to recruit JAZ repressors for degradation. The downstream transcription factors MYC2/3/4 and ERF1/ORA59 are released, activating biosynthesis of defense compounds, defensins and GS, respectively. In response to pathogen infection and herbivore feeding, BES1 functions in the plant growth-defense trade off by negatively regulating JA-induced transcription of *PDF1.2*s and indole-GS biosynthetic genes, which helps restore the proper cellular levels of defensin and GS.

expression (Li et al., 2009; Wang et al., 2018). By contrast, upon binding to BRRE elements, BES1 attenuates the expression of BR-repressed genes by interacting with the transcriptional corepressor MYB-LIKE2 (MYBL2; Ye et al., 2012). Consistent with these findings, our results indicate that BES1 suppresses the transcription of indole-GS biosynthetic genes (*CYP79B3* and *UGT74B1*) by interacting with GS-related MYBs (MYB34, MYB51, and MYB122). These findings support the idea that BES1 functions with other MYB transcription factors as cofactors to positively or negatively regulate gene expression.

CONCLUSION

Based on the findings from this study and several previous works, we propose the following model (Fig. 8). Plant growth signals trigger the expression of genes, including *DWE1/ROT3*, to induce BR biosynthesis (Choe, 2006; Ohnishi et al., 2006). BR binds to the cell-surface receptor kinase BRI1 to activate BR signal transduction by sequential transphosphorylation events (Li et al., 2002; Yin et al., 2002; Li and Deng, 2005; Sun et al., 2010). Subsequently, the dephosphorylated transcription factor BES1 translocates from the cytoplasm into the nucleus, leading to the expression of BR-responsive genes and promotion of plant growth and development (Wang et al., 2012).

By contrast, insect attack and necrotrophic pathogen infection induce the accumulation of JAs. The active JA form, JA-Ile, is perceived by the COI1 receptor to recruit JAZ repressors for degradation (Chini et al., 2007; Thines et al., 2007; Yan et al., 2009). The downstream transcription factors MYC2/3/4 and ERF1/ORA59 are released to activate the biosynthesis of defense compounds GS and defensins, respectively (Pré et al., 2008; Zarei et al., 2011; Pieterse et al., 2012; Schweizer et al., 2013).

Particularly, upon pathogen infection and herbivore feeding, BES1 plays a negative role in antagonizing the JA-induced transcription of *PDF1.2s* and indole-GS biosynthetic genes (Fig. 8; Guo et al., 2013). This process helps restore the elevated levels of defensin and GS to homeostatic cellular levels, thereby functioning in the plant growth-defense tradeoff. Moreover, the interaction between BES1 and indolic GS-related MYBs is essential for the regulation of BES1-suppressed transcription of GS biosynthetic genes (Fig. 8). Given the importance of the interplay among JA, SA, ET, and ABA in the regulation of plant defense responses, it would be interesting to further investigate how these hormones coordinate with BR to maintain cellular homeostasis during or after plant interactions with pathogens and insect herbivores.

MATERIALS AND METHODS

Plant Materials, Growth Conditions, and Treatments

All wild type, mutant, and transgenic lines used in this study are in the Columbia ecotype (Col-0) background. The following mutants were described previously: *bes1-2* (Kang et al., 2015), *bes1-D* (Vilarrasa-Blasi et al., 2014; Yin et al., 2002), *bzr1-1D* (Wang et al., 2002), *coi1-2* (Xu et al., 2002), and *35S::BES1-L-GFP* (Jiang et al., 2015). The T-DNA insertion mutants with the locus names *rot3-2* (CS3728), and *bzr1-1D* (CS65987) described in this study were obtained from The Arabidopsis Information Resource (http://www.arabidopsis.org). The *dwe1 coi1-2* mutant was generated by crossing *dwe1* with *coi1-2*, and homozygous plants were identified through PCR-based genotyping and sequencing of the F2 population.

After being surface sterilized with 20% (v/v) bleach containing 0.1% (v/v) Tween 20 for 20 min and washed five times with sterilized water, seeds were germinated on Murashige and Skoog (MS) medium (Sigma-Aldrich) containing 1% (w/v) Suc and 0.8% (w/v) agar. Following stratification for 3 d at 4°C in the dark, the plates were transferred to a growth cabinet with a 16-h-light/8-h-dark (20°C–24°C) photoperiod and incubated for 9 d. The seedlings were subsequently transplanted to soil for further growth.

Map-Based Cloning of DWE1

To map *dwe1*, we crossed *dwe1* (in the Columbia background) with wild type Landsberg *erecta* (L*er*). The F1 plants self-fertilized to generate the F2 population.

In the segregating F2 population, plants with *dwe1* morphology were used for linkage analysis.

For the complementation test, the 1575 bp CDS of *ROT3* was amplified by PCR using the wild-type complementary DNA (cDNA) as a template. Primers used for amplification of *ROT3* are listed in Supplemental Table S2. To express the Myc-FLAG-ROT3 fusion protein under the control of 35S promoter, the cDNA fragment, with an N-terminal FLAG tag, was cloned into the binary vector pCXSN-Myc. The construct was transformed into *Agrobacterium tumefaciens* and subsequently introduced into the *dwe1* mutant by floral dipping (Clough and Bent, 1998). Transformants (*dwe1::35S:ROT3*) were selected by hygromycin, and their transcription level of *ROT3* was confirmed by RT-qPCR analysis.

Construction of Plasmids and Generation of Transgenic Plants

To generate transgenic lines, the CDS of *PDF1.2a* was amplified and constructed into a modified pCAMBIA1301 binary vector (driven by the *35S* promoter and fused with a 3× FLAG tag, then digested with *Sac*I and *Mlu*I) to generate the *PDF1.2a-3FLAG* construct. The constructs were then transformed into Col-0 wild-type plants using the *Agrobacterium tumefaciens*-mediated floral-dip method to obtain *PDF1.2a-OE* transgenic plants. *PDF1.2a-OE* was crossed with the *bes1-D* mutant to obtain *PDF1.2a-OE bes1- D* double mutants.

To construct an expression vector for recombinant BES1 protein, the full-length CDS of *BES1* was amplified from Arabidopsis (*Arabidopsis thaliana*) cDNA and inserted into the pRSET A vector (Invitrogen) and then digested with *Bam*HI and *Hind*III, resulting in the *6His-BES1* construct.

For the transient expression assay, the coding fragments of *BES1*, *ERF1*, *ORA59*, *MYC2*, *MYB34*, *MYB51*, and *MYB122* were inserted into the *Bam*HI-*Stu*I site of *pHBT-35SPPDK-2HA* or *pHBT-35SPPDK-2FLAG* vectors, resulting in the effectors *35S::BES1-HA*, *35S::ERF1-FLAG*, *35S::ORA59-FLAG*, *35S::MYC2-FLAG*, *35S::MYB34-FLAG*, *35S::MYB51-FLAG*, and *35S::MYB122-FLAG*, respectively. To generate the reporter constructs, the ~2000-bp promoter sequence of each target gene was PCR amplified and inserted into the cloning site (*Kpn*I/*Bam*HI) of the pGreenII 0800-LUC vector (Hellens et al., 2005). To construct the *p1.2a-TAA+-LUC* reporter, the *TAA+* fragment of *PDF1.2a* was produced using the primers *p1.2a-TAA+-LUC*-F/R and *pfu* DNA polymerase, and the fragment was inserted into *p1.2a-LUC* digested with *Spe*I and *Sac*II. The promoter sequence of *PDF1.2b* was PCR amplified using the primers *p1.2b-TAA+-LUC*-F/R and inserted into *1.2b TAA+-LUC* (digested with *Kpn*I), resulting in the reporter construct *p1.2b-TAA+-LUC*.

Insect Herbivory and Pathogen Infection

Insect feeding and pathogen inoculation were carried out as previously described (Hu et al., 2013) with minor modifications. For each genotype, 60 first-instar *Spodoptera exigua* larvae were reared on 10 4-week-old plants. At 7 d after feeding, all living *S. exigua* larvae (more than 30 larvae for each genotype) were removed from the plants and collected for weighing and photographing. All experiments were repeated three times independently with similar results.

The fungal pathogen *Botrytis cinerea* was maintained on potato dextrose agar medium at room temperature. Spore masses were collected and suspended in inoculation buffer (20 mM K_2HPO_4 [pH 5.7], 20 mM NH_4NO_3 [pH 5.7], 1 mM $MgSO_4$, 10 mM $CaCl_2$, 50 mM Suc [pH 5.7], and 10 mM sodium citrate). More than 15 mature rosette leaves per genotype from 4-week-old plants were placed in petri dishes containing 0.6% (w/v) agar and sealed with adhesive tape. For each leaf, 5-μL droplets containing ~1.25×10^6 spores/mL *B. cinerea* suspension were inoculated and incubated in the dark for 3 d, followed by a 16-h-light/8-h-dark photoperiod at 20°C to 24°C. The lesion diameter (mm) was calculated using ImageJ software. All experiments were repeated three times with similar results.

RNA Extraction and RT-qPCR Analysis

Seven-day-old seedlings grown on MS medium (>30 seedlings per genotype) were transferred to and drenched in 100 μM MeJA, 100 μM MeJA, and 200 nM BL (Sigma-Aldrich, cat. no. E1641; MeJA + BL), or water (control). After 6 h of treatment, total RNA was extracted from the seedlings using the HiPure plant RNA mini kit according to the manufacturer's instructions, and cDNA was synthesized using a HiScript II Q RT SuperMix kit with gDNA Wiper (Vazyme). RT-qPCR was conducted with a StepOne Plus real-time PCR system (Applied Biosystems) using ChamQ SYBR color qPCR master mix (Vazyme). The conditions for RT-qPCR were an initial step for 2 min at 95°C, followed by 40 cycles of 10 s at 95°C, 15 s at 55°C, and 30 s at 72°C. The relative expression levels of the target genes were calculated using the $2^{-\Delta\Delta Ct}$ method following the manufacturer's instructions. *ACTIN2* was used as an internal control. Specific primers (listed in Supplemental Table S2) were designed (based on their DNA sequences) to PCR amplify *PDF1.2* (Hu et al., 2013) and genes involved in regulating GS synthesis (Guo et al., 2013). Quantification was performed using three technical replicates. Experiments were repeated three times with similar results.

SEM Analysis

SEM was performed as described previously (Ahlstrand, 1996) using samples frozen in liquid nitrogen and examined on a cold stage. Leaves of 3-week-old plants were plated in gold and observed under a Hitachi S-3400N scanning election microscope at 20 and 15 kV. The number of stomata in leaves was measured using ImageJ software. Experiments were repeated three times independently with similar results.

Protein-DNA Binding Assays

The ChIP-qPCR assay was performed as described previously using 12-d-old *BES1-L-GFP* seedlings (Jiang et al., 2015) treated with 1 μM BL for 2 h (Yuan et al., 2017). After coating with anti-GFP antibodies (Invitrogen) or anti-IgG (CST), the protein/DNA complexes were immunoprecipitated with Dynabeads Protein G (Invitrogen). The *ACT2* promoter was used as a negative control. Real-time PCR was performed with immunoprecipitated DNA using the StepOne Plus real-time PCR system (Applied Biosystems) and the specific primers listed in Supplemental Table S2. Quantification was performed using three technical replicates. Experiments were repeated three times with similar results.

For EMSA, the recombinant His-BES1 protein was expressed in *Escherichia coli* BL21 (DE3) cells (Vazyme) and purified using Ni-NTA agarose (Invitrogen). EMSA was performed using a LightShift chemiluminescent EMSA kit (Thermo Scientific) according to the manufacturer's instructions and as described previously (Yuan et al., 2017). Synthetic DNA oligonucleotide probes labeled with biotin were incubated with purified His-BES1 recombinant protein in the presence or absence of excess amounts of unlabeled competitors or unlabeled mutated probes for 30 min at room temperature. The biotin-labeled DNA fragments were used as biotin probe. The biotin-unlabeled DNA fragments of the same sequences were used as the competitors (Cold Probe). The fragments with BES1-binding sites were mutated to AAAAAA were used as Cold mProbe. The 200× and 500× mean the amounts of Cold Probe and Cold mProbe were 200- and 500-fold to that of biotin probe. The sequences of the oligonucleotides used in this assay are listed in Supplemental Table S2.

Measurement of LUC Activity

All reporter constructs used in this study were generated with the pGreenII 0800-LUC vector (Hellens et al., 2005), and the effector constructs were generated using the pHBT construct driven by the *35SPPDK* promoter. The primers used to produce these constructs are listed in Supplemental Table S2. The preparation and transformation of wild-type (Col-0) protoplasts were performed as described previously (Yoo et al., 2007). Firefly LUC and Renilla LUC (REN) activities were measured using the Dual-Luciferase Reporter Assay System (Promega) and the SpectraMax i3x Multi-Mode Detection Platform (Molecular Devices). Relative LUC activity was expressed as the ratio of LUC to REN. All experiments were independently repeated three times with similar results. For each assay, three technical replicates were analyzed.

CoIP and BiFC Assays

For CoIP assay, the full-length CDS of BES1 and MYBs were cloned upstream of an HA tag or FLAG tag, respectively, driven by the *UBQ10* promoter. The constructs used for transient expression analysis were purified using a Maxi kit (Magen). Arabidopsis mesophyll protoplast preparation and transfection were performed according to Yoo et al. (2007). Four-week-old wild-type protoplasts were transfected with the indicated plasmids and cultured for 16 h for protein expression. The cells were collected and lysed in immunoprecipitation buffer (10 mM HEPES [pH 7.4], 150 mM NaCl, 2 mM EDTA, and 10% [v/v] glycerol) with 0.5% (v/v) Triton for total protein extraction. 10% (v/v) of the total lysate

was used for input, and the remaining lysate was incubated with FLAG affinity beads (Sigma-Aldrich) for 5 h at 4°C. The beads were collected and washed five times with immunoprecipitation buffer containing 0.1% (v/v) Triton. The immunoprecipitates were eluted into 40 μL 2× SDS loading buffer at 95°C for 10 min and separated by 10% (w/v) SDS-PAGE for detection with anti-FLAG (Sigma-Aldrich, cat. no. A8592, 1:5000) and anti-HA antibodies (Sigma-Aldrich, cat. no. H6533, 1:5000).

For BiFC assay, the full-length CDS of BES1 was cloned upstream of a split cYFP driven by the *UBQ10* promoter. The full-length CDS of MYBs were cloned upstream of a split nYFP driven by the *35SPPDK* promoter. The split nYFP and cYFP plasmids were coexpressed in leaf protoplasts for 16 h and the YFP signal was detected by confocal microscopy.

GS Measurements

To measure GS levels, 4-week-old plants were treated for 3 d with five neonate *S. exigua* larvae per plant, untreated plants were used as controls. GSs were extracted and detected as described previously (Glauser et al., 2012) with minor modifications. Frozen leaf samples (200 mg) were ground with a glass rod in 1.975 mL ice-cold MeOH/H_2O (70:30, v/v) and incubated at 80°C for 15 min. The homogenate was centrifuged at 3500*g* for 10 min at 4°C, and the supernatant was filtered through a 0.45-μm filter for analysis. Ultra-high-performance liquid chromatography/quadrupole time-of-flight (UHPLC-Q-TOF) analysis was performed on an Acquity UPLC system (Shimadzu) interfaced to a 5600 plus Q-TOF (SCIEX) with electrospray ionization. Aliphatic and indolic GSs were identified by matching the precursor ion and ion fragments of each compound (Glauser et al., 2012). Aliphatic and indolic GSs were quantified relatively based on peak area using sinigrin as an internal standard as described previously (Guo et al., 2013; Miao et al., 2013). The amount of each GS was determined by the following formula: (peak area of the GS × the molar amount of corresponding internal standard signigrin)/(peak area of the corresponding internal standard in that sample × the weight of fresh plant tissue). The GS content was expressed as nmol/g of fresh weight of Arabidopsis seedlings. Quantification was performed using four technical replicates. Experiments were repeated twice with similar results (for one experiment, eight plants were used for each genotype).

Microarray Analysis

Microarray analysis was carried out according to Xie et al. (2015). Four-week-old wild-type (Col-0) and *dwe1* mutant rosettes were harvested. Each sample included three biological replicates, and each replicate was collected from three independent plants. Total RNA was extracted by the RNeasy plant mini kit (Qiagen) following the manufacturer's instructions. Affymetrix ATH1 Arabidopsis chips (Affymetrix) were used for labeling, hybridization, scanning, and detection. Affymetrix Gene Chip software MAS 5.0 and GeneSpring 12.6 (Agilent) were used in raw data collection, normalization, and DEG identification, followed by the criterion of fold change more than 1.5-fold and $P < 0.05$. DAVID (http://david.abcc.ncifcrf.gov/; Dennis et al., 2003) was used to classify the DEG groups, and R language was applied for calculations and figure plots.

Accession Numbers

Sequence data from this article can be found in the GenBank/EMBL data libraries under the following accession numbers: *ROT3* (AT4G36380), *PDF1.2a* (AT5G44420), *PDF1.2b* (AT2G26020), *VSP1* (AT5G24780), *VSP2* (AT5G24770), *BES1* (AT1G19350), *MYC2* (AT1G32640), *ORA59* (AT1G06160), *ERF1* (AT3G23240), *MYB34* (AT5G60890), *MYB51* (AT1G18570), *MYB122* (AT1G74080), *MYB28* (AT5G61420), *MYB29* (AT5G07690), *MYB76* (AT5G07700), *ARF4* (AT5G60450), *CYP79B2* (AT4G39950), *CYP79B3* (AT2G22330), *CYP79F1* (AT1G16410), *CYP83A1* (AT4G13770), *CYP83B1* (AT4G31500), *UGT74B1* (AT1G24100), *SUR1* (AT2G20610), and *ACTIN2* (AT3G18780).

Supplemental Data

The following supplemental materials are available.

Supplemental Figure S1. Gene Ontology term enrichment analysis (DAVID) of DEGs in *dwe1* mutant.

Supplemental Figure S2. Complementation of *dwe1* mutation by BL application.

Supplemental Figure S3. Genetic complementation of the *dwe1* mutant.

Supplemental Figure S4. BES1 inhibits *PDF1.2a* and *PDF1.2b* expression.

Supplemental Figure S5. Overexpression of *PDF1.2a* rescues the sensitivity of *bes1-D* to *B. cinerea* infection, but not to *S. exigua* herbivory.

Supplemental Figure S6. BES1 is not associated with aliphatic GS biosynthesis.

Supplemental Figure S7. BES1 is involved in regulation of GS biosynthesis.

Supplemental Figure S8. BES1 negatively regulates GS synthesis by interacting with indolic GS biosynthesis genes and MYB transcription factors.

Supplemental Table S1. Microarray data showing the genes differentially expressed in *dwe1*.

Supplemental Table S2. Primers and oligonucleotide probes used in this study.

ACKNOWLEDGMENTS

The authors thank the Arabidopsis Biological Resource Center (www.arabidopsis.org) for providing *rot3-2* (CS3727) and *bzr1-1D* (CS65987), Daoxin Xie (Tsinghua University) for the *coi1-2* seeds, and Xuelu Wang (Huazhong Agricultural University) for the *BES1-L-GFP* and *bes1-D* seeds.

Received October 7, 2019; accepted November 14, 2019; published November 27, 2019.

LITERATURE CITED

Ahlstrand G (1996) Low-temperature low-voltage scanning microscopy (LTLVSEM) of uncoated frozen biological materials: a simple alternative. In G Bailey, J Corbett, R Dimlich, J Michael, and N Zaluzec, eds, Proceedings of Microscopy Microanalysis. San Francisco Press, San Francisco, CA, pp 918–919

Albrecht C, Boutrot F, Segonzac C, Schwessinger B, Gimenez-Ibanez S, Chinchilla D, Rathjen JP, de Vries SC, Zipfel C (2012) Brassinosteroids inhibit pathogen-associated molecular pattern-triggered immune signaling independent of the receptor kinase BAK1. Proc Natl Acad Sci USA **109:** 303–308

Bednarek P, Piślewska-Bednarek M, Svatoš A, Schneider B, Doubský J, Mansurova M, Humphry M, Consonni C, Panstruga R, Sanchez-Vallet A, et al (2009) A glucosinolate metabolism pathway in living plant cells mediates broad-spectrum antifungal defense. Science **323:** 101–106

Belkhadir Y, Jaillais Y, Epple P, Balsemão-Pires E, Dangl JL, Chory J (2012) Brassinosteroids modulate the efficiency of plant immune responses to microbe-associated molecular patterns. Proc Natl Acad Sci USA **109:** 297–302

Brown RL, Kazan K, McGrath KC, Maclean DJ, Manners JM (2003) A role for the GCC-box in jasmonate-mediated activation of the *PDF1.2* gene of Arabidopsis. Plant Physiol **132:** 1020–1032

Campos ML, de Almeida M, Rossi ML, Martinelli AP, Litholdo Junior CG, Figueira A, Rampelotti-Ferreira FT, Vendramim JD, Benedito VA, Peres LE (2009) Brassinosteroids interact negatively with jasmonates in the formation of anti-herbivory traits in tomato. J Exp Bot **60:** 4347–4361

Chen S, Andreasson E (2001) Update on glucosinolate metabolism and transport. Plant Physiol Biochem **39:** 743–758

Chini A, Fonseca S, Fernández G, Adie B, Chico JM, Lorenzo O, García-Casado G, López-Vidriero I, Lozano FM, Ponce MR, et al (2007) The JAZ family of repressors is the missing link in jasmonate signalling. Nature **448:** 666–671

Choe S (2006) Brassinosteroid biosynthesis and inactivation. Physiol Plant **126:** 539–548

Chung HS, Howe GA (2009) A critical role for the TIFY motif in repression of jasmonate signaling by a stabilized splice variant of the JASMONATE ZIM-domain protein JAZ10 in Arabidopsis. Plant Cell **21:** 131–145

Clay NK, Adio AM, Denoux C, Jander G, Ausubel FM (2009) Glucosinolate metabolites required for an *Arabidopsis* innate immune response. Science **323:** 95–101

Clough SJ, Bent AF (1998) Floral dip: a simplified method for *Agrobacterium*-mediated transformation of *Arabidopsis thaliana*. Plant J **16:** 735–743

Dennis G Jr., Sherman BT, Hosack DA, Yang J, Gao W, Lane HC, Lempicki RA (2003) DAVID: Database for annotation, visualization, and integrated discovery. Genome Biol **4:** 3

Fernández-Calvo P, Chini A, Fernández-Barbero G, Chico JM, Gimenez-Ibanez S, Geerinck J, Eeckhout D, Schweizer F, Godoy M, Franco-Zorrilla JM, et al (2011) The Arabidopsis bHLH transcription factors MYC3 and MYC4 are targets of JAZ repressors and act additively with MYC2 in the activation of jasmonate responses. Plant Cell **23:** 701–715

Franco-Zorrilla JM, López-Vidriero I, Carrasco JL, Godoy M, Vera P, Solano R (2014) DNA-binding specificities of plant transcription factors and their potential to define target genes. Proc Natl Acad Sci USA **111:** 2367–2372

Frerigmann H, Gigolashvili T (2014) MYB34, MYB51, and MYB122 distinctly regulate indolic glucosinolate biosynthesis in *Arabidopsis thaliana*. Mol Plant **7:** 814–828

Gampala SS, Kim TW, He JX, Tang W, Deng Z, Bai MY, Guan S, Lalonde S, Sun Y, Gendron JM, et al (2007) An essential role for 14-3-3 proteins in brassinosteroid signal transduction in *Arabidopsis*. Dev Cell **13:** 177–189

Gan L, Wu H, Wu D, Zhang Z, Guo Z, Yang N, Xia K, Zhou X, Oh K, Matsuoka M, et al (2015) Methyl jasmonate inhibits lamina joint inclination by repressing brassinosteroid biosynthesis and signaling in rice. Plant Sci **241:** 238–245

Gigolashvili T, Engqvist M, Yatusevich R, Müller C, Flügge UI (2008) HAG2/MYB76 and HAG3/MYB29 exert a specific and coordinated control on the regulation of aliphatic glucosinolate biosynthesis in *Arabidopsis thaliana*. New Phytol **177:** 627–642

Gigolashvili T, Yatusevich R, Berger B, Müller C, Flügge UI (2007) The R2R3-MYB transcription factor HAG1/MYB28 is a regulator of methionine-derived glucosinolate biosynthesis in *Arabidopsis thaliana*. Plant J **51:** 247–261

Glauser G, Schweizer F, Turlings TC, Reymond P (2012) Rapid profiling of intact glucosinolates in *Arabidopsis* leaves by UHPLC-QTOFMS using a charged surface hybrid column. Phytochem Anal **23:** 520–528

Gudesblat GE, Russinova E (2011) Plants grow on brassinosteroids. Curr Opin Plant Biol **14:** 530–537

Guo R, Qian H, Shen W, Liu L, Zhang M, Cai C, Zhao Y, Qiao J, Wang Q (2013) BZR1 and BES1 participate in regulation of glucosinolate biosynthesis by brassinosteroids in *Arabidopsis*. J Exp Bot **64:** 2401–2412

He JX, Gendron JM, Sun Y, Gampala SS, Gendron N, Sun CQ, Wang ZY (2005) BZR1 is a transcriptional repressor with dual roles in brassinosteroid homeostasis and growth responses. Science **307:** 1634–1638

Hellens RP, Allan AC, Friel EN, Bolitho K, Grafton K, Templeton MD, Karunairetnam S, Gleave AP, Laing WA (2005) Transient expression vectors for functional genomics, quantification of promoter activity and RNA silencing in plants. Plant Methods **1:** 13

Howe GA, Jander G (2008) Plant immunity to insect herbivores. Annu Rev Plant Biol **59:** 41–66

Howe GA, Major IT, Koo AJ (2018) Modularity in jasmonate signaling for multistress resilience. Annu Rev Plant Biol **69:** 387–415

Hu P, Zhou W, Cheng Z, Fan M, Wang L, Xie D (2013) *JAV1* controls jasmonate-regulated plant defense. Mol Cell **50:** 504–515

Huang Y, Han C, Peng W, Peng Z, Xiong X, Zhu Q, Gao B, Xie D, Ren C (2010) Brassinosteroid negatively regulates jasmonate inhibition of root growth in Arabidopsis. Plant Signal Behav **5:** 140–142

Jiang J, Zhang C, Wang X (2015) A recently evolved isoform of the transcription factor BES1 promotes brassinosteroid signaling and development in *Arabidopsis thaliana*. Plant Cell **27:** 361–374

Kang S, Yang F, Li L, Chen H, Chen S, Zhang J (2015) The Arabidopsis transcription factor BRASSINOSTEROID INSENSITIVE1-ETHYL METHANESULFONATE-SUPPRESSOR1 is a direct substrate of MITOGEN-ACTIVATED PROTEIN KINASE6 and regulates immunity. Plant Physiol **167:** 1076–1086

Katsir L, Schilmiller AL, Staswick PE, He SY, Howe GA (2008) COI1 is a critical component of a receptor for jasmonate and the bacterial virulence factor coronatine. Proc Natl Acad Sci USA **105:** 7100–7105

Li J, Wen J, Lease KA, Doke JT, Tax FE, Walker JC (2002) BAK1, an *Arabidopsis* LRR receptor-like protein kinase, interacts with BRI1 and modulates brassinosteroid signaling. Cell **110:** 213–222

Li L, Deng XW (2005) It runs in the family: regulation of brassinosteroid signaling by the BZR1-BES1 class of transcription factors. Trends Plant Sci **10:** 266–268

Li L, Yu X, Thompson A, Guo M, Yoshida S, Asami T, Chory J, Yin Y (2009) Arabidopsis MYB30 is a direct target of BES1 and cooperates with BES1 to regulate brassinosteroid-induced gene expression. Plant J **58:** 275–286

Major IT, Yoshida Y, Campos ML, Kapali G, Xin XF, Sugimoto K, de Oliveira Ferreira D, He SY, Howe GA (2017) Regulation of growth-defense balance by the JASMONATE ZIM-DOMAIN (JAZ)-MYC transcriptional module. New Phytol **215:** 1533–1547

Martínez C, Espinosa-Ruíz A, de Lucas M, Bernardo-García S, Franco-Zorrilla JM, Prat S (2018) PIF4-induced BR synthesis is critical to diurnal and thermomorphogenic growth. EMBO J **37:** e99552

Miao H, Wei J, Zhao Y, Yan H, Sun B, Huang J, Wang Q (2013) Glucose signalling positively regulates aliphatic glucosinolate biosynthesis. J Exp Bot **64:** 1097–1109

Miyaji T, Yamagami A, Kume N, Sakuta M, Osada H, Asami T, Arimoto Y, Nakano T (2014) Brassinosteroid-related transcription factor BIL1/BZR1 increases plant resistance to insect feeding. Biosci Biotechnol Biochem **78:** 960–968

Mylne J, Botella JR (1998) Binary vectors for sense and antisense expression of Arabidopsis ESTs. Plant Mol Biol Rep **16:** 257–262

Ning Y, Liu W, Wang GL (2017) Balancing immunity and yield in crop plants. Trends Plant Sci **22:** 1069–1079

Nolan T, Chen J, Yin Y (2017) Cross-talk of Brassinosteroid signaling in controlling growth and stress responses. Biochem J **474:** 2641–2661

Ohnishi T, Szatmari AM, Watanabe B, Fujita S, Bancos S, Koncz C, Lafos M, Shibata K, Yokota T, Sakata K, et al (2006) C-23 hydroxylation by *Arabidopsis* CYP90C1 and CYP90D1 reveals a novel shortcut in brassinosteroid biosynthesis. Plant Cell **18:** 3275–3288

Peng Z, Han C, Yuan L, Zhang K, Huang H, Ren C (2011) Brassinosteroid enhances jasmonate-induced anthocyanin accumulation in *Arabidopsis* seedlings. J Integr Plant Biol **53:** 632–649

Pieterse CM, Van der Does D, Zamioudis C, Leon-Reyes A, Van Wees SC (2012) Hormonal modulation of plant immunity. Annu Rev Cell Dev Biol **28:** 489–521

Pré M, Atallah M, Champion A, De Vos M, Pieterse CM, Memelink J (2008) The AP2/ERF domain transcription factor ORA59 integrates jasmonic acid and ethylene signals in plant defense. Plant Physiol **147:** 1347–1357

Ren C, Han C, Peng W, Huang Y, Peng Z, Xiong X, Zhu Q, Gao B, Xie D (2009) A leaky mutation in *DWARF4* reveals an antagonistic role of brassinosteroid in the inhibition of root growth by jasmonate in Arabidopsis. Plant Physiol **151:** 1412–1420

Robert-Seilaniantz A, Grant M, Jones JD (2011) Hormone crosstalk in plant disease and defense: more than just jasmonate-salicylate antagonism. Annu Rev Phytopathol **49:** 317–343

Schweizer F, Fernández-Calvo P, Zander M, Diez-Diaz M, Fonseca S, Glauser G, Lewsey MG, Ecker JR, Solano R, Reymond P (2013) Arabidopsis basic helix-loop-helix transcription factors MYC2, MYC3, and MYC4 regulate glucosinolate biosynthesis, insect performance, and feeding behavior. Plant Cell **25:** 3117–3132

Sheard LB, Tan X, Mao H, Withers J, Ben-Nissan G, Hinds TR, Kobayashi Y, Hsu FF, Sharon M, Browse J, et al (2010) Jasmonate perception by inositol-phosphate-potentiated COI1-JAZ co-receptor. Nature **468:** 400–405

Shin SY, Chung H, Kim SY, Nam KH (2016) *BRI1-EMS-suppressor* 1 gain-of-function mutant shows higher susceptibility to necrotrophic fungal infection. Biochem Biophys Res Commun **470:** 864–869

Staswick PE, Su W, Howell SH (1992) Methyl jasmonate inhibition of root growth and induction of a leaf protein are decreased in an *Arabidopsis thaliana* mutant. Proc Natl Acad Sci USA **89:** 6837–6840

Sun Y, Fan XY, Cao DM, Tang W, He K, Zhu JY, He JX, Bai MY, Zhu S, Oh E, et al (2010) Integration of brassinosteroid signal transduction with the transcription network for plant growth regulation in *Arabidopsis*. Dev Cell **19:** 765–777

Sun Y, Li P, Shen D, Wei Q, He J, Lu Y (2019) The *Ralstonia solanacearum* effector RipN suppresses plant PAMP-triggered immunity, localizes to the endoplasmic reticulum and nucleus, and alters the NADH/NAD^+ ratio in *Arabidopsis*. Mol Plant Pathol **20:** 533–546

Thines B, Katsir L, Melotto M, Niu Y, Mandaokar A, Liu G, Nomura K, He SY, Howe GA, Browse J (2007) JAZ repressor proteins are targets of the SCF^{COI1} complex during jasmonate signalling. Nature **448:** 661–665

Thomma BP, Cammue BP, Thevissen K (2002) Plant defensins. Planta **216:** 193–202

Vilarrasa-Blasi J, González-García MP, Frigola D, Fàbregas N, Alexiou KG, López-Bigas N, Rivas S, Jauneau A, Lohmann JU, Benfey PN, et al (2014) Regulation of plant stem cell quiescence by a brassinosteroid signaling module. Dev Cell **30:** 36–47

Wang J, Wu D, Wang Y, Xie D (2019) Jasmonate action in plant defense against insects. J Exp Bot **70:** 3391–3400

Wang W, Lu X, Li L, Lian H, Mao Z, Xu P, Guo T, Xu F, Du S, Cao X, et al (2018) Photoexcited CRYPTOCHROME1 interacts with dephosphorylated BES1 to regulate Brassinosteroid signaling and photomorphogenesis in Arabidopsis. Plant Cell **30:** 1989–2005

Wang ZY, Bai MY, Oh E, Zhu JY (2012) Brassinosteroid signaling network and regulation of photomorphogenesis. Annu Rev Genet **46:** 701–724

Wang ZY, Nakano T, Gendron J, He J, Chen M, Vafeados D, Yang Y, Fujioka S, Yoshida S, Asami T, et al (2002) Nuclear-localized BZR1 mediates brassinosteroid-induced growth and feedback suppression of brassinosteroid biosynthesis. Dev Cell **2:** 505–513

Wasternack C, Hause B (2013) Jasmonates: Biosynthesis, perception, signal transduction and action in plant stress response, growth and development. An update to the 2007 review in *Annals of Botany*. Ann Bot **111:** 1021–1058

Xiao S, Dai L, Liu F, Wang Z, Peng W, Xie D (2004) COS1: An Arabidopsis coronatine insensitive1 suppressor essential for regulation of jasmonate-mediated plant defense and senescence. Plant Cell **16:** 1132–1142

Xie DX, Feys BF, James S, Nieto-Rostro M, Turner JG (1998) COI1: an *Arabidopsis* gene required for jasmonate-regulated defense and fertility. Science **280:** 1091–1094

Xie LJ, Chen QF, Chen MX, Yu LJ, Huang L, Chen L, Wang FZ, Xia FN, Zhu TR, Wu JX, et al (2015) Unsaturation of very-long-chain ceramides protects plant from hypoxia-induced damages by modulating ethylene signaling in Arabidopsis. PLoS Genet **11:** e1005143

Xu L, Liu F, Lechner E, Genschik P, Crosby WL, Ma H, Peng W, Huang D, Xie D (2002) The SCF^{COI1} ubiquitin-ligase complexes are required for jasmonate response in Arabidopsis. Plant Cell **14:** 1919–1935

Yan J, Zhang C, Gu M, Bai Z, Zhang W, Qi T, Cheng Z, Peng W, Luo H, Nan F, et al (2009) The *Arabidopsis* CORONATINE INSENSITIVE1 protein is a jasmonate receptor. Plant Cell **21:** 2220–2236

Yan Y, Shen L, Chen Y, Bao S, Thong Z, Yu H (2014) A MYB-domain protein EFM mediates flowering responses to environmental cues in *Arabidopsis*. Dev Cell **30:** 437–448

Yang DH, Hettenhausen C, Baldwin IT, Wu J (2011) BAK1 regulates the accumulation of jasmonic acid and the levels of trypsin proteinase inhibitors in *Nicotiana attenuata*'s responses to herbivory. J Exp Bot **62:** 641–652

Yant L, Mathieu J, Dinh TT, Ott F, Lanz C, Wollmann H, Chen X, Schmid M (2010) Orchestration of the floral transition and floral development in *Arabidopsis* by the bifunctional transcription factor APETALA2. Plant Cell **22:** 2156–2170

Ye H, Li L, Guo H, Yin Y (2012) MYBL2 is a substrate of GSK3-like kinase BIN2 and acts as a corepressor of BES1 in brassinosteroid signaling pathway in *Arabidopsis*. Proc Natl Acad Sci USA **109:** 20142–20147

Yin Y, Vafeados D, Tao Y, Yoshida S, Asami T, Chory J (2005) A new class of transcription factors mediates brassinosteroid-regulated gene expression in *Arabidopsis*. Cell **120:** 249–259

Yin Y, Wang ZY, Mora-Garcia S, Li J, Yoshida S, Asami T, Chory J (2002) BES1 accumulates in the nucleus in response to brassinosteroids to regulate gene expression and promote stem elongation. Cell **109:** 181–191

Yoo SD, Cho YH, Sheen J (2007) *Arabidopsis* mesophyll protoplasts: a versatile cell system for transient gene expression analysis. Nat Protoc **2:** 1565–1572

Yu MH, Zhao ZZ, He JX (2018) Brassinosteroid signaling in plant-microbe interactions. Int J Mol Sci **19:** e4091

Yu X, Li L, Zola J, Aluru M, Ye H, Foudree A, Guo H, Anderson S, Aluru S, Liu P, et al (2011) A brassinosteroid transcriptional network revealed by genome-wide identification of BESI target genes in *Arabidopsis thaliana*. Plant J **65:** 634–646

Yuan LB, Dai YS, Xie LJ, Yu LJ, Zhou Y, Lai YX, Yang YC, Xu L, Chen QF, Xiao S (2017) Jasmonate regulates plant responses to postsubmergence reoxygenation through transcriptional activation of antioxidant synthesis. Plant Physiol **173:** 1864–1880

Zarei A, Körbes AP, Younessi P, Montiel G, Champion A, Memelink J (2011) Two GCC boxes and AP2/ERF-domain transcription factor ORA59 in jasmonate/ethylene-mediated activation of the *PDF1.2* promoter in Arabidopsis. Plant Mol Biol **75:** 321–331

Zhai Q, Yan L, Tan D, Chen R, Sun J, Gao L, Dong MQ, Wang Y, Li C (2013) Phosphorylation-coupled proteolysis of the transcription factor MYC2 is important for jasmonate-signaled plant immunity. PLoS Genet **9:** e1003422

Zhang L, Zhang F, Melotto M, Yao J, He SY (2017) Jasmonate signaling and manipulation by pathogens and insects. J Exp Bot **68:** 1371–1385

Zhou M, Memelink J (2016) Jasmonate-responsive transcription factors regulating plant secondary metabolism. Biotechnol Adv **34:** 441–449